

Dielectric Elastomer Generators: Recent Advances in Materials, Electronic Circuits, and Prototype Developments

Krishna Veer Singh Gurjar, Anup Sankar Sadangi, Ajeet Kumar, Dilshad Ahmad,*
Karali Patra,* Ieuan Collins, Mokarram Hossain, Rafic M. Ajaj, and Yahya Zweiri

The ongoing climate crisis requires innovative methods to maximize renewable and sustainable energy resources. There have been advancements in harvesting energy from ambient motions such as wind, ocean waves, and human movements. Dielectric elastomer generators (DEGs) are a promising option for energy harvesting due to their high energy density and compatibility with low-frequency oscillations. This review provides an in-depth overview of DEGs, including electroactive materials, electromechanical characterization, electronics for harvesting, interfacing circuits, prototypes, and challenges. DEGs have the potential to play a significant role in decarbonizing energy for both small- and large-scale applications using ambient energy sources.

1. Introduction


One of the most profound and urgent challenges facing both present and future generations is climate change. The over-reliance on nonrenewable energy sources such as coal, oil, and

K. V. S. Gurjar, A. Kumar, K. Patra
Department of Mechanical Engineering
Indian Institute of Technology Patna
Patna 801106, India
E-mail: kpatra@iitp.ac.in

D. Ahmad, R. M. Ajaj, Y. Zweiri
Advanced Research and Innovation Center (ARIC)
Department of Aerospace Engineering
Khalifa University of Science and Technology
127788 Abu Dhabi, United Arab Emirates
E-mail: dilshad.ahmad@ku.ac.ae

I. Collins, M. Hossain
Zienkiewicz Institute for AI
Data and Modelling
Faculty of Science and Engineering
Bay Campus
Swansea University Swansea
SA1 8EN Swansea, UK

A. S. Sadangi
Department of ECE
Gayatri Vidya Parisad College of Engineering
Visakhapatnam-48, India

 The ORCID identification number(s) for the author(s) of this article can be found under <https://doi.org/10.1002/aesr.202400221>.

© 2024 The Author(s). Advanced Energy and Sustainability Research published by Wiley-VCH GmbH. This is an open access article under the terms of the Creative Commons Attribution License, which permits use, distribution and reproduction in any medium, provided the original work is properly cited.

DOI: 10.1002/aesr.202400221

natural gas has led to severe environmental repercussions, including accelerated global warming and ecological disruption. A 2020 report by the World Energy Council underscores the precariousness of our current energy landscape, projecting that oil and gas reserves could be exhausted before the end of the century.^[1] This situation is compounded by a dramatic increase in annual CO₂ emissions, which have surged from 18 billion tonnes to an alarming 33.7 billion tonnes over the last four decades. Despite this stark reality, nonrenewable resources still dominate global energy consumption, accounting for ≈85% of the

total. This underlines an urgent and critical need to transition swiftly and effectively to sustainable and renewable energy sources. Exploring and harnessing alternative energy sources such as solar, wind, ocean waves, and human motion represents a crucial step toward reducing our carbon footprint and ensuring a resilient and sustainable energy future. This review focuses on dielectric elastomer generators (DEGs), a burgeoning technology that offers promising solutions for capturing ambient energy and contributes significantly to the global effort of decarbonizing energy systems.

Renewable energy technologies have been exploring alternative energy sources like radio frequency, solar, temperature gradients, vibration, wind, ocean waves, and even human motion, as depicted in **Figure 1**.^[2,3] While Hydropower, solar energy, and wind energy have become economically feasible in recent years, other sources of mechanical energy such as ocean waves,^[4–7] human motions,^[8–10] and building/bridge vibrations^[11,12] have remained largely untapped. Harvesting electrical energy from ambient motions using electromagnetic, piezoelectric, and soft dielectric elastomers has shown significant promise for both large- and small-scale applications.^[13–15]

In electromagnetic energy harvesting method, an altering magnetic field induces a voltage in the conductor. Although the electromagnetic method has the advantages of improved reliability and reduced mechanical damping, electromagnetic materials are bulky and difficult to integrate with microelectronic devices.^[16] In contrast, piezoelectric materials (especially PZT thin film) are better candidates for electrical energy harvesting using external mechanical energy.^[16] These materials are crystalline, enabling them to transform electrical energy from mechanical strain and vice versa. Piezoelectric ceramics can generate electricity from mechanical pressure, but they have some limitations, such as the use of undesirable lead compounds and the requirement of high-frequency energy. Additionally, they are

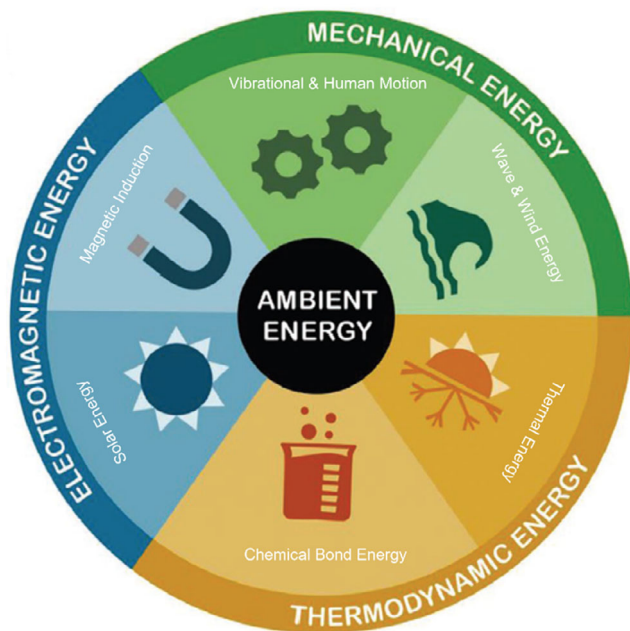


Figure 1. Ambient sources of energy available for harvesting: mechanical energy (vibrations, human motion, wave energy, and wind energy), electromagnetic energy (solar energy, magnetic induction), and thermodynamic energy (thermal energy and chemical bond energy).^[15]

rather stiff, thus connecting them to energy sources requires a strong, rigid structure.^[17] However, low-frequency energy generation can be made possible using an electrostatic generator based on charged soft polymeric dielectrics.

DEGs offer a way to capture low-frequency motion energy from human motion or vibrations of buildings, bridges, and other structures.^[18–22] These generators are soft, deformable, and have a high energy density, allowing them to be attached to intricate structures like the human body, to collect extra mechanical energy.^[23–26] For example, DEGs implemented into

soft/rubbery heel-strike generators have been found to generate more power from heel-strike motions than those based on the piezoelectric element which is more complex, expensive, and heavier.^[27,28] Dielectric elastomers are highly extensible variable capacitors, making them perfect for obtaining energy from complex movements due to their lightweight and soft characteristics.^[29,30]

Figure 2 illustrates the process by which electrical energy is converted from mechanical energy: 1) First, stretching of elastomer results in a closer distance between the electrodes; 2) a charge is applied to this stretched configuration; 3) as the elastomer is relaxed the electrodes get farther apart changing the capacitance, subsequently the voltage must increase due to the charge remaining constant; and 4) the gain in electrical energy is harvested.

The electrical energy harvested is directly proportional to the deformation of the generator, making it desirable to maximize the extent of the stretch.^[31]

The literature contains a limited number of review articles discussing the applications and theory of dielectric elastomers as a working medium for energy harvesting.^[32] For example, in 2010, Suo et al.^[33] investigated the theory of dielectric elastomers based on empirical observations related to continuum mechanics and thermodynamics. They also explained the correlation between nonlinear and nonequilibrium characteristics, such as viscoelasticity and electromechanical instability, when the material is subjected to a large deformation and electric potential. Also, Kornbluh et al.^[31] presented a short review of different energy harvester prototypes and lifetime issues of DEGs. Romasanta et al.^[34] reviewed various ways to improve the harvesting and actuation capabilities of dielectric elastomers. Madsen et al.^[35] presented an extensive review of silicone-based commercial dielectric elastomers, polymer blends, elastomers with conductive fillers, and chemically modified elastomers for transducer applications. More recently, Moretti et al.^[36] reviewed the most recent developments in the power electronics, design of hardware architectures, and controls for DEGs concerning the various application targets, including small-scale systems like ambient vibration energy harvesters or human motion energy harvesters

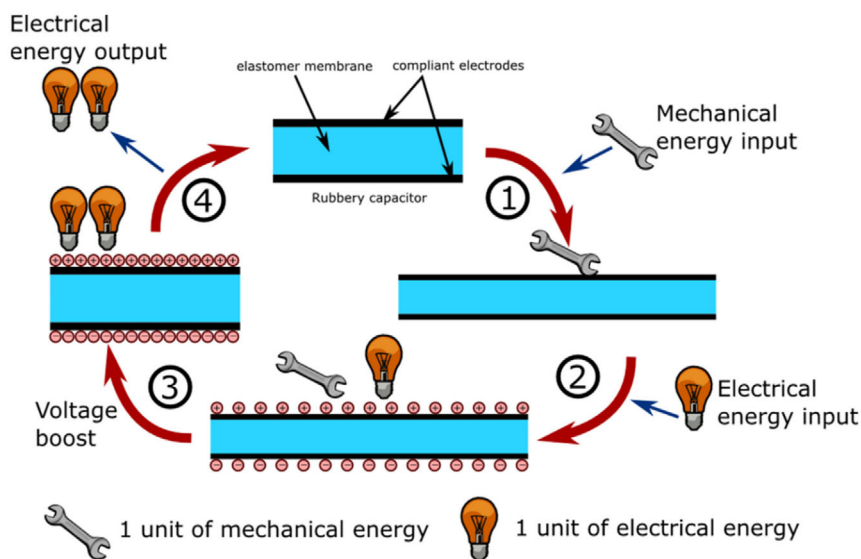


Figure 2. Schematic of a DEG energy cycle.^[228]

and large-scale systems like ocean wave energy converters (WECs). Chiba et al.^[37] reviewed various working prototypes of power generators using DEGs and their prospects, such as megawatt scale wave energy harvesters. Collins et al.^[38] reviewed the advancements in material choices, and methods for modeling cutting-edge membrane-based WECs. Very recently, Di et al.^[39] reviewed the working principle, materials, parameters, and deformation modes of DEGs along with the preexisting prototypes for both small and large-scale applications.

The current review article aims to thoroughly investigate several crucial aspects of DEGs, focusing on recent advancements and emerging trends. A significant area of this review is the synthesis of novel composites that combine dielectric elastomers with conductive fillers and polymer blends. These innovations enhance the material's energy-harvesting performance by improving its mechanical properties, electrical conductivity, and overall efficiency. We delve into how these new formulations and processing techniques pave the way for more effective and versatile DEGs.

In addition to material advancements, the review addresses the latest developments in energy conversion circuits and interfacing technologies. We explore the different energy conversion circuits that have been studied to optimize efficiency, including advancements in rectification, voltage regulation, and power management. Furthermore, the review highlights innovations in interfacing circuits, which are crucial for integrating DEGs with electronic devices to ensure efficient energy transfer and improved performance. The review also provides an in-depth analysis of the mechanical and electrical properties affecting the performance of DEGs. We examine how factors such as elasticity, dielectric strength, and material composition impact energy conversion and harvesting efficiency. By highlighting these properties, we offer insights into their influence on device design and application. A key contribution of this review is its comparative analysis of various deformation modes used during the energy harvesting process. We evaluate different strategies, such as uniaxial, biaxial, and planar stretching, and assess their

efficiency and effectiveness in optimizing energy capture from ambient sources. This analysis provides valuable guidance for selecting the most suitable deformation modes for various applications. Furthermore, while numerous reviews have covered the theory, applications, and prototypes of DEGs, there remains a critical need for a thorough examination of the state-of-the-art in materials, energy conversion circuits, control circuits, and design innovations. This review aims to fill this gap by offering a comprehensive overview of current challenges and potential solutions for the widespread adoption of DEGs. We address issues such as durability, susceptibility to adverse conditions, and the need for high operating voltages. Additionally, the review explores future research and development prospects, providing a roadmap for advancing DEG technology.

The article is structured as follows: Section 2 covers the latest developments in dielectric elastomers with conducting fillers and polymer blends designed to enhance energy harvesting. Section 3 focuses on energy conversion and interfacing circuits utilized to improve harvesting efficiency. Section 4 discusses the electromechanical properties of DEGs and various deformation modes used in energy harvesting. Section 5 presents and compares recent prototypes developed for applications such as human motion, wave energy, and wind energy harvesting. Finally, Section 6 addresses the challenges faced in dielectric material-based energy harvesting and explores future prospects for this technology.

2. Types of Elastomers Used as DEGs

The choice of elastomer is crucial for the performance of a DEG, with a wide range trialed so far,^[40] see **Figure 3**. Many of these are commercially available rubbers that have been used in designing prototype DEGs.^[41] Most of the reviews conducted till now generally cover commercially available elastomers for harvesting applications, also very few of them have reported the use of elastomer composites. Our work presents a detailed and comparative review of all kinds of dielectric elastomer like commercially available dielectric elastomer,

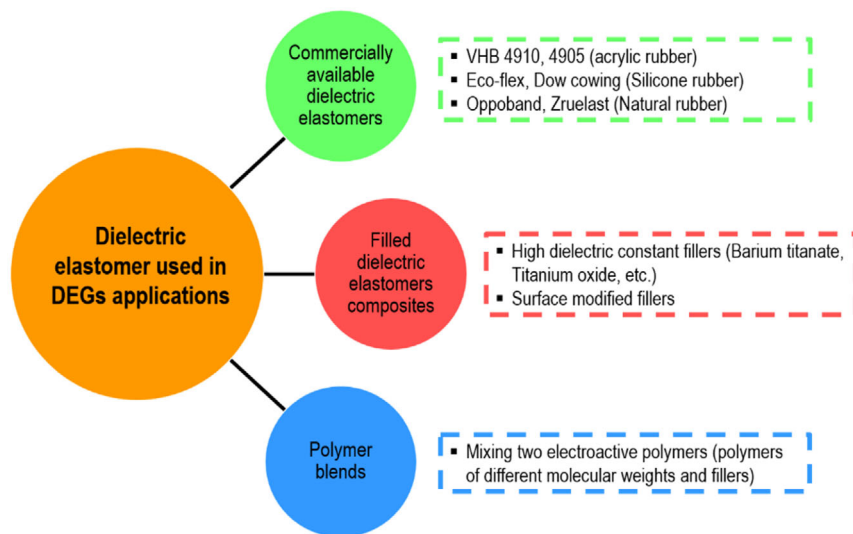


Figure 3. Different types of dielectric elastomers and their composites.

filled dielectric elastomer composites, and polymer blends. The novel materials like elastomer composites and polymer blends have shown great advantages over the commercially available dielectric elastomers in terms of improved dielectric constant, breakdown strength, and better elastic modulus.

2.1. Commercially Available Dielectric Elastomeric Materials

Acrylic elastomers (e.g., very high bond (VHB)), silicone elastomers (e.g., Ecoflex, elastosil), and natural rubber (e.g., Oppoband) have desirable electromechanical properties which make them promising materials for the DEG applications.^[42,43] Commercially available VHB (3M, USA) consists of a vinyl group and terminates with carboxylic acids.^[44,45] The dielectric constant of VHB is 5.5 at 1 Hz, it also has high breakdown strength and excellent electromechanical properties.^[46–48] However, its large hysteresis, long stress relaxation time, adhesive nature, and sensitivity to environmental conditions are unwanted for energy harvesting applications.^[49–51] Silicone^[52,53] is another commonly used elastomer that consists of a backbone chain of silicone and oxygen.^[54,55] It has a low elastic modulus due to the Si–O bond, low dielectric constant, and moderate electromechanical properties. Additionally, it has advantageous properties such as a wide temperature range for applications, comparatively low viscoelastic behavior, as well as low moisture absorption properties.^[56] Another common elastomer is natural rubber which consists of the monomer of isoprene. Natural rubbers have comparatively low dielectric constants, high dielectric breakdown strengths, low hysteresis, and low dielectric losses.^[57] Many of these commercial elastomers have been applied to energy-harvesting prototypes. For reference, Jiang et al. developed a cone-shaped DEG using commercially available VHB 4910, optimizing the energy harvesting performance in the equal-biaxial mode of stretching, which demonstrates a maximum electromechanical conversion efficiency of 40% and a peak energy density of 130 mJ g⁻¹.^[58] Moretti et al. prepared commercially available silicone rubber and custom-prepared compliant electrode, which suggested 173 mJ g⁻¹ of energy density and 30% of conversion efficiency, see Figure 4. Kaltseis et al. reported high power densities of 200 mW g⁻¹ and high energy densities of 369 mJ g⁻¹ using commercially available natural rubber, suggesting it is the best candidate for energy harvesting applications, as shown in Figure 4.^[11]

2.2. Elastomer Composites for DEGs

The main limitation of energy conversion in DEGs using commercially available dielectric elastomers is their limited electromechanical properties, i.e., low breakdown strength, significant dielectric losses, and low dielectric constant.^[59] Therefore, various research works have focused on the synthesis of novel materials having large deformation (low elastic modulus and high elongation at break) with improved dielectric constants, and optimistic electromechanical properties.^[60–67] For instance, Bortot et al.^[68,69] improved the dielectric elastomer composite's performance by adding ceramic fillers to a silicone polymer matrix. They prepared two composites of silicone polymer matrix by using ferroelectric ceramic fillers: lead zirconate-titanate (PZT) and lead magnesium niobate–lead titanate (PMN–PT).

They noted an increase in both composites' dielectric constant. The mechanical properties, however, were negatively impacted; the dielectric breakdown strength decreased, and the elastic modulus increased with increasing filler concentration. The energy harvesting performance increased by 61.3% and 63.2% for PMN–PT and PZT fillers, respectively. Yin et al.^[70,71] synthesized polyurethane-based dielectric elastomer composites with dibutyl phthalate (DBP) as plasticizers and barium titanate (BT) as filler to improve the dielectric constant and electromechanical properties. They reported that the PU composites with 60 phr of DBP and 25 phr of BT had a 43% decrease in the elastic modulus and a 28% increase in the dielectric constant. Furthermore, they observed an energy harvesting density of 1.71 mJ cm⁻³ and an efficiency of 0.45%, as illustrated in Figure 5.

Bele et al. prepared silicone composites with titanium oxide (TiO₂) nanotubes which act as a filler for the Polydimethylsiloxane- α , ω -diol (PDMS) composite.^[72] They observed both a change in mechanical and dielectric properties when adding and increasing the concentration of TiO₂ nanotubes. For instance, the elastic modulus for unfilled silicone rubber was 0.26 MPa, but this increased to 0.4 and 0.5 MPa for TiO₂ nanotubes of 2–5% by total weight, respectively. Similarly, at the same concentrations, the dielectric constant improved from 7.75 to 11.6 at 0.1 Hz. The maximum energy efficiency was found to be 8.84% for the TiO₂ nanotube-based silicone composite. Contrary to previous findings, Yang et al.^[73] observed a reduction in mechanical properties when using a solution-casting method to prepare polyurethane (PU) composites. This decreased the overall elastic modulus of the composite but increased its elongation at break. They used surface-modified barium titanate (BT) nanoparticles as filler particles, which involved a surface modification process with 4,4-diphenylmethane diisocyanate (MDI), as illustrated in Figure 5.^[73] Through the synthesis process, they saw a rise in the dielectric constant as high as 8 at 1 Hz with the addition of 6% of filler content by weight and an elongation at break as high as 1070%. To investigate energy harvesting performance, they reported a conversion efficiency of 1.56% and an energy conversion density of 2.88 mJ cm⁻³ at 900 V.^[74]

To improve the mechanical, dielectric, and mechano-electroconversion properties, Zhang et al.^[61] fabricated a surface-modified copper calcium titanate (CCTO) filled silicone composite. The surface modification of CCTO enhanced the inorganic and polymer materials' interfacial interaction, resulting in improved dispersion and enhanced dielectric properties, as illustrated in Figure 5. To explore its potential as a DEG material, they investigated the composite elastomer's capacity to harvest electrical power using a cone-type energy harvester. The 26 wt% CCTO (polydopamine-modified) integrated composite produced twice as much energy as the pure polymer matrix. Concerning energy conversion efficiency, the 20% by weight CCTO composite elastomer showed a maximum of 3.36%, which was 68% higher than that of the pure matrix.

2.3. Polymer Blends

Polymer blends are the combination of two or more dielectric elastomers, so the resulting elastomer will have combined and improved properties of both of its parent elastomers.^[75,76]

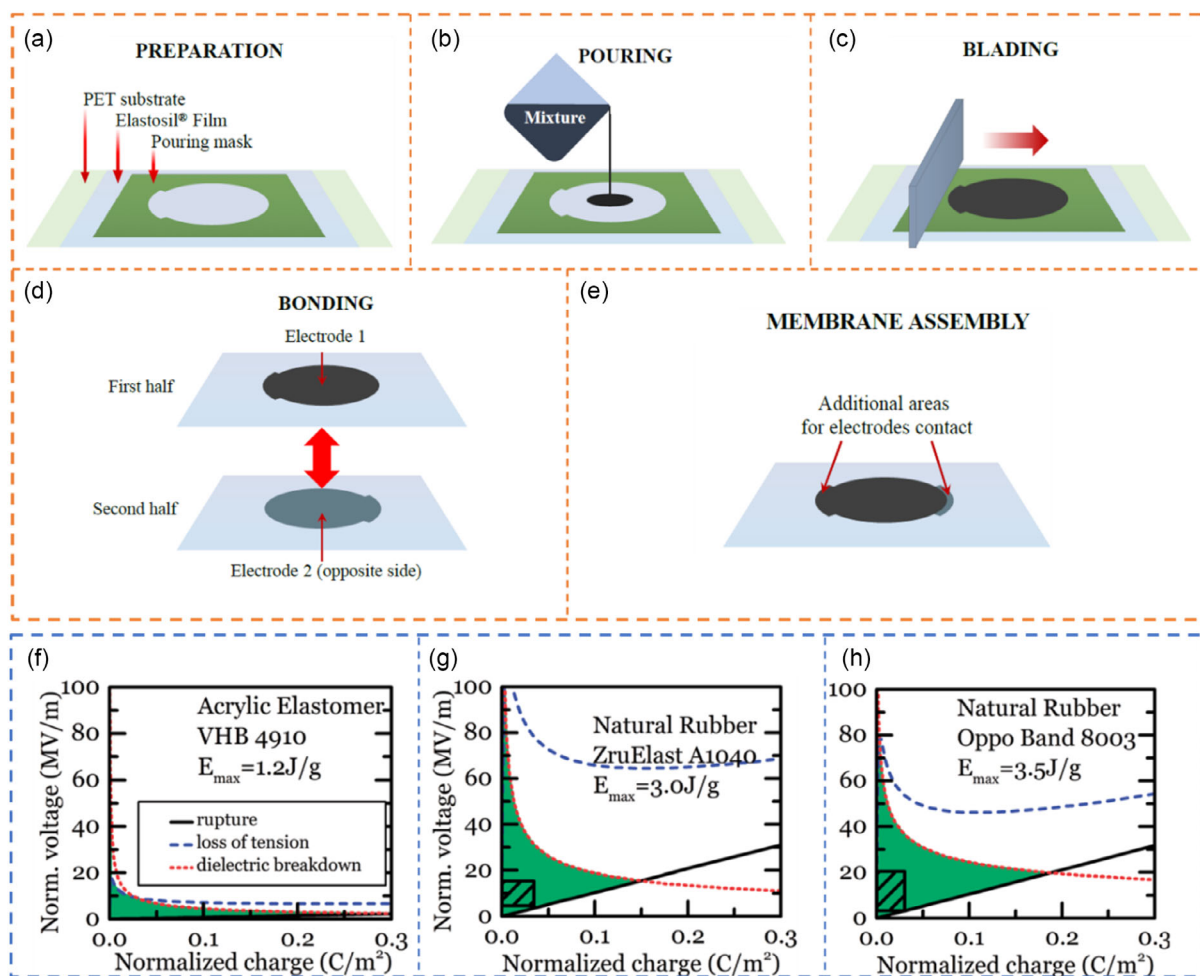


Figure 4. Different phases for preparing the flexible electrode on elastomer: a) On the elastosil film, a pouring mask with a patterned cut is placed; b) a solution of isopropanol, carbon black (CB), and polydimethylsiloxane (PDMS) is poured; c) process of blading removes extra material; d) crosslinking results in the bonding of two membranes; e) electrode-coated membrane is completed.^[229] f–h) The comparison of the maximum possible harvested energy (green area) for VHB 4910, Zruelast A1040 (natural rubber), and Oppo Band 8003 (natural rubber). The hatched rectangle displays the actual energy conversion cycle of the experiment in (g,h).^[11]

In a recent study, Ellingford et al.^[77] fabricated self-healing dielectric elastomer blend of poly (styrene-butadiene-styrene) (SBS) and methyl-3-mercaptopropionate (M3M) by a grafting technique. The resulting material exhibited a mechanical strain of 1000% and a low dielectric loss of 0.03 and a dielectric constant of 7.5. By using a diaphragm-type energy harvester, an energy density of 11 mJ g^{-1} was obtained.

In another recent study, Gong et al.^[78] used a straightforward one-step procedure, in which highly polar azobenzene molecules were chemically grafted onto a network of hydroxyl-terminated polydimethylsiloxane (PDMS) to produce molecularly homogeneous silicone rubber, as demonstrated in **Figure 6**. They also added dimethyl silicone oil (DMSO) as a plasticizer to reduce elastic modulus of resulting material. As shown in **Table 1**, the resulting azo-g-PDMS/DMSO films were simultaneously improved in terms of their breakdown strength and dielectric constant, all the while maintaining a relatively low elastic modulus. Subsequently, conical mode of deformation was used to

optimize the material's energy harvesting ability, resulting in a high electromechanical conversion efficiency of 5.01% and a high energy harvesting density of 0.69 mJ cm^{-3} .

Gallone et al.^[79] created a mixture of polyurethane and PDMS by combining a moisture-cured polymer with a two-component polyurethane elastomer (poly 74 from Polytek Development) and a commercial three-component PDMS-based formulation (TC-5005 A/B/C by BJB Enterprises Inc.). The dielectric permittivity of a blend made with 40 vol% polyurethane ranged from 5.2 at high frequencies (1 kHz) to 15.5 at low frequencies (10 Hz), thus, suggesting a higher permittivity than pure polyurethane (6.5 at low frequencies). In a separate study, Risse et al.^[80] created a mixture of a PDMS matrix and 2300 g mol^{-1} cyanopropyl-functional PDMS, in which the cyanofunctional PDMS functioned as a plasticizer and blend. They observed that the dielectric permittivity doubled from its initial value. Using a conical membrane setup, they achieved a 3.5% conversion efficiency and an energy density of 0.4 mJ g^{-1} .

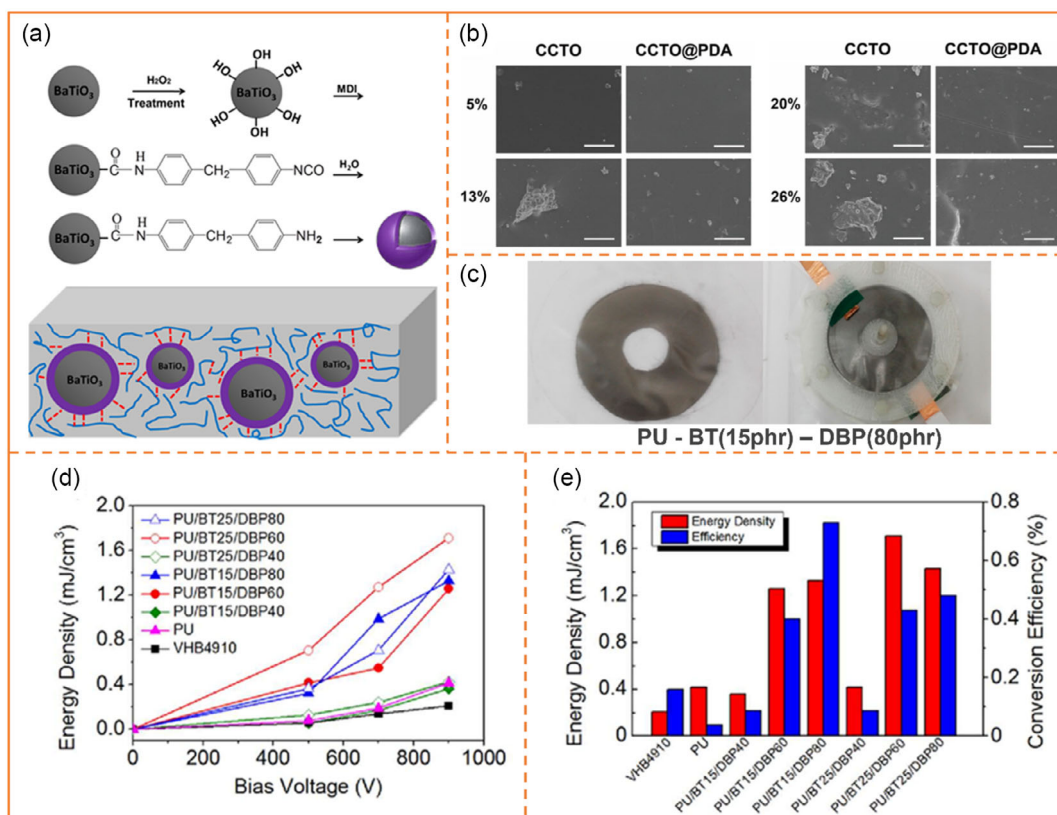


Figure 5. a) Schematic illustration of the BT-MDI preparation process and the BT-MDI/PU composite film microstructure. The blue lines represent the PU molecules, while the red dashed lines show the H bonds that connect MDI and PU chains,^[73] b) scanning electron microscopy photos of the composites' cross-sections include CCTO and CCTO@PDA particles at varying mass concentrations. Scale bar: 30 μm ,^[61] c) membrane image of polyurethane (PU) filled with 15 phr of BT and 80 phr of DBP,^[70] d) energy density per cubic volume versus bias voltage graph for different dielectric elastomeric films, and e) graph for energy density per cubic volume and conversion efficiency of various dielectric elastomeric films under 80% of areal expansion, 1000 mm min^{-1} , of constant tensile release rate, and 900 V of bias voltage.^[70]

2.4. Flexible Electrode Materials for DEGs

Electrodes are a crucial part of dielectric DE-energy harvesters. They work as the positive and negative terminal of a flexible parallel plate capacitor. A good electrode material should possess good charge conductivity, low ohmic resistance, and good compliance with the elastomer membrane. Much of the DEG application conducted thus far, utilizes carbon grease (CG) as the predominant electrode material. However, recent studies have focused on enhancing the compliance between the electrode and the elastomer membrane, leading to significant improvements in electrode durability. These advancements aim to optimize the mechanical and electrical properties of the electrodes, ensuring better performance and longevity in practical applications. Hubertus et al.^[81] prepared thin film nickel-based wrinkled flexible electrodes by sputtering the 10–20 nm layer of nickel on a biaxially prestretched silicone elastomer membrane. These electrodes possess low ohmic resistance that is 2 orders of magnitude lower than CB-based electrodes, and these electrodes were able to withstand 200% of areal strain and 10 million cycles of mechanical stretching while remaining electrically conductive.

Zang et al.^[82] in 2021, synthesized a hydrogen bond cross-linked supramolecular network of silicone rubber (SiR–SN)

and subsequently incorporated a commercially available, highly conductive CB and CG into the SiR–SN matrix. The addition of CG and CB significantly enhanced the electrical conductivity and stability of conductivity at high strain. The energy loss was reduced by 83.5%, and harvested energy density (23 mJ cm^{-3}) was increased by 73.1% by using a flexible electrode made of SiR–SN matrix containing 5 phr of CB and 60 phr of CG.

Ding et al.^[83] prepared thin flexible electrodes of CB evenly dispersed in the polydimethylsiloxane (PDMS) matrix. High electrical conductivity, good compliance, and high elongation at break were successfully obtained. The energy loss was reduced by 40.3%, and harvested energy density (20.3 mJ cm^{-3}) was increased by 32% compared to CG-coated DEG. These flexible electrodes were able to withstand 60 000 cycles of stretching under 200% of strain.

Zang et al.^[84] in 2024, synthesized a flexible electrode consisting of multiple dynamic bond crosslinked supramolecular networks (Ns) and liquid metal (LM). These flexible electrodes show high conductivity ($16\,000 \text{ S cm}^{-1}$), self-healing capability at room temperature, and charge loss reduction by 3 order of magnitude.

Yao et al.^[85] prepared flexible electrodes made out of a mixture of silicone rubber (100 phr) with CG (40 phr) and CB (5 phr) and

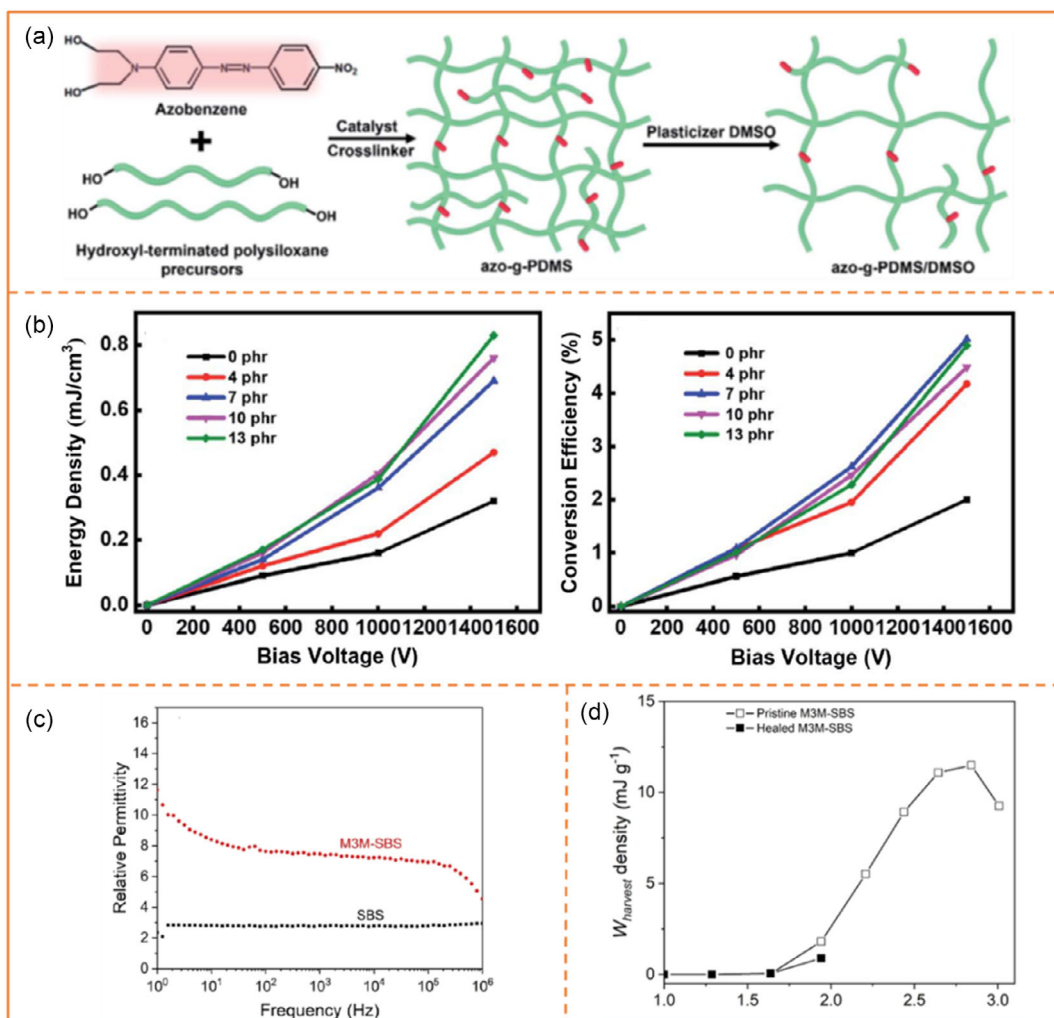


Figure 6. a) An azo-g-PDMS/DMSO manufacturing process, b) with varying azobenzene loading levels, the azo-g-PDMS/DMSO's volumetric energy density and mechano-electrical conversion efficiency with respect to the bias voltage.^[75] c) comparison of relative permittivity of SBS-M3M polymer blend with pure SBS polymer, and d) harvested energy variation with stretching of elastomer membrane for SBS-M3M polymer blend.^[77]

vulcanizing agent tetraethyl orthosilicate (5, 10, and 20 wt% of uncured silicone rubber) named SRE-1, SRE-2, and SRE-3, respectively, based on the amount of vulcanizing agent presence. This combination reduced the fractional resistance at the interface between the dielectric elastomer and the electrode, allowing for smoother electrical conduction and minimizing localized stress concentrations at the interface. This improved electrical and mechanical coupling was found to extend the fatigue life of the dielectric elastomer by 20.3 times compared to traditional electrode materials.

3. Electronics for Energy Conversion and Interfacing

3.1. Electronics for DEGs

To develop a robust energy generator, it is important to have an efficient power-conditioning unit. Power-conditioning systems

are considered powerful tools for understanding the behavior of the energy harvesting system.^[86,87] Only a limited number of review articles have covered the electronics aspect of dielectric elastomer (DE)-based energy harvesting. They have only reviewed the conversion cycles and basic conversion circuits. Our work aims to extensively cover all types of conversion and interfacing circuits of DE-based energy harvesting systems. Our work has comparatively reviewed the latest conversion and interfacing circuits like self-priming circuits, frequency-dependent interfacing circuits, interfacing circuits with potential dividers, and interfacing circuits with dynamic metal oxide semiconductor field effect transistor (MOSFET) switches.

The electromechanical transformation using a DEG is characterized by energy conversion cycles under the charge–voltage (Q – V) plane, electrical–mechanical plane, and the Maxwell stress–stretch plane.^[41,60,88–90] Among these energy conversion cycles, the Q – V cycle is considered to describe the energy conversion pattern with triangular and rectangular cycles.^[91,92]

Table 1. Comparison of dielectric properties and energy harvesting performance of DE materials.

Type of DE material	Material specification	Filler content	Dielectric constant	Dielectric loss	Dielectric breakdown strength [MV m]	Elongation at break [%]	Elastic modulus [MPa]	Harvested energy [mJ g ⁻¹]	Energy efficiency [%]
Commercially available dielectric elastomers	VHB 4910 ^[58]	–	4.3 (1 kHz)	0.025	69	1200	0.1	130	40
	Silicone rubber ^[229]	–	2.85 (1 kHz)	0.0056	120	400	0.25	173	30
	Natural rubber ^[11]	–	3.2 (1 kHz)	0.002	97	800	0.1–1	369	30
Filled dielectric elastomer composites	PU/BT ^[70]	BT (15%)	8.3 (1 Hz)	0.075 (1 Hz)	59.9	615	11.6	1.78	45.00
	PDMS/TiO ₂ ^[72]	TiO ₂ (2%)	7.75 (0.1 Hz)	38.1 (0.1 Hz)	62.0	617	0.92	1.36	8.84
	PU/BT-MDI ^[73]	BT (6%)	8.4 (1 kHz)	0.018 (10 ³ Hz)	82	–	–	3.01	1.56
	PDMS/CCTO/PDA ^[61]	CCTO/PDA (26%)	5.55 (1 kHz)	0.009	42	–	–	0.71	3.36
Polymer blends	SBS/M3M ^[77]	95% (GF) ^{a)}	7.5 (1 kHz)	0.03	39.5	1000	2.4	11	–
	PDMS/cyanopropyl functional copolymer ^[80]	40% cyanopropyl functional PDMS	9 (1 kHz)	0.25 (0.1 Hz)	22	270	0.25	0.4	3.5
	azo-g PDMS/DMSO ^[75]	Azobenzene (7 phr)	4.34 (1 kHz)	0.025 (1 kHz)	73	–	0.45	0.71	5.01

^{a)}Grafting ratios.

Several signal processing units have been reported to process the generated electrical signal. Maximum delivery of the generated energy to the load is ensured by the signal processing unit.^[92–94] The conditioning circuits used so far can be categorized based on their invention and adoption. A comprehensive summary of the circuits used over the past decade and their pros and cons are provided in **Table 2**. The circuits, known as interfacing circuits for DEGs, are responsible for a controlled flow of charges pumped by the cyclic movement of the DEG transducer.^[95]

The charge–voltage (Q – V) plane is the most effective method to depict the phenomenon of energy conversion. The transducer's electromechanical state is assessed inside this plane. The review on DEG-based energy harvesting reveals the two most prominent geometries for its characterization, such as

triangular^[96,97] and rectangular.^[36,98] The area of the Q – V cycle loop is numerically equal to the amount of energy converted in a single cycle of a DEG's periodic mechanical motion.^[89,99] Stretching the electrode-coated DE sample starts the cycle, which is then followed by the application of priming voltage. The process is completed when the stretched sample relaxes in an open circuit condition.

When the elastomer membrane is stretched (Point B), the associated capacitance with the DEG achieves its maximum value (C_{max}), and the DEG is primed with an initial voltage V_{bias} , while the charge with it on the Q_s plane. This is equivalent to path A–B in **Figure 7b**. As the elastomer contracts, the related capacitance begins to decline (C_{min}) until the DE film is totally relaxed (Point C). The charge stays constant because the DE is relaxed

Table 2. Various interfacing circuits along with their pros and cons.

Sl no.	Approach made by	Interfacing circuit	Advantages	Disadvantages
1	Chiba et al. ^[37]	High-voltage probe	Low-design complexity	High measurement error and power losses
2	Jiangshui et al. ^[231]	Potential divider	No external supply required	Low efficient circuit
3.	J. Huang et al. ^[237] and McKay et al. ^[111]	Zener regulator	Required only one component	Low output current at the load
4.	Wang et al. ^[238]	Buck converter	High energy efficient	Required external source
5	Jurgen et al. ^[239]	Bidirectional converter	Does not require a Booster.	Multiple numbers of MOSFET required, External source
6	Jurgen et al. ^[162] and Ramanuja et al. ^[116]	Fly-back converter	Low voltage switching and high efficiency	Due to transformer use fabrication is difficult

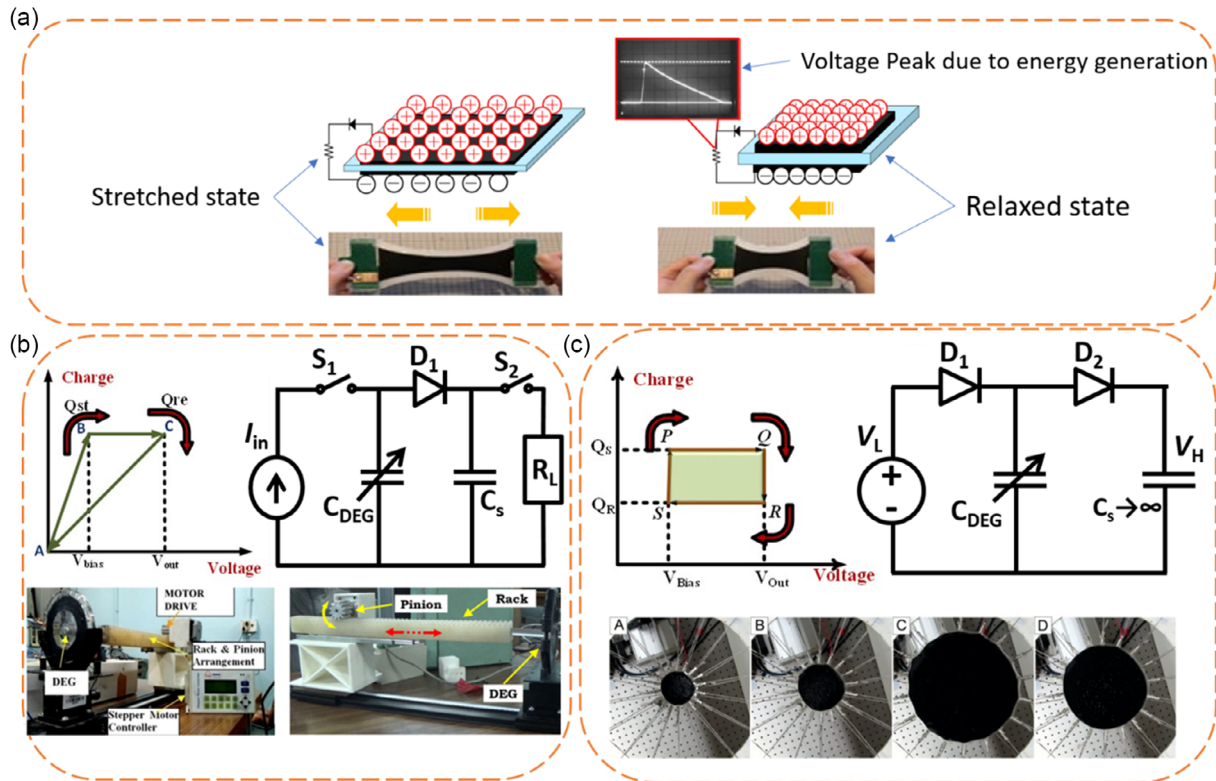


Figure 7. a) Operating principle of a DE-based power generation showing charge distribution on DEG membrane in the stretched and unstretched state then work done by the contracting elastomer is converted into electrical energy,^[2] b) triangular conversion cycle and circuit diagram with conical stretching prototype which utilizes triangular conversion cycle,^[131,230] and c) rectangular conversion cycle and circuit diagram along with the biaxial prototype showing various steps of conversion cycle.^[231,232]

in an electrically isolated environment. The relaxation follows the path segment B-C. The voltage increases to V_{out} as a result of the change from a high capacitance to a low capacitance at a fixed charge. The charge at point C is Q_{re} , and it returns through the path C-A. The area of the geometry included within ABC can be used to define how much energy is generated, with the converted energy given as

$$E_{hav} = \frac{1}{2} C_{min} V_{out}^2 - \frac{1}{2} C_{max} V_{bias}^2 \quad (1)$$

In contrast to the triangular conversion cycle, in the case of applied mechanical excitation, the electrode-coated DE sample undergoes deformation, as a result of which the electrode area is increased and the DE thickness is decreased, causing the capacitance associated with DEG to reach its maximum value. The DEG is then connected to bias voltage V_{Bias} , and the charge associated with DEG is Q_s corresponding to the point “P” in Figure 7c. As the DE relaxes, the capacitance begins to decline until the elastomer is entirely relaxed and reaches point “Q” where the capacitance change occurs. Since electrical isolation is used during the relaxation of DE, the charge along path P-Q remains constant. The transducer capacitance reaches a minimum value when the charge at point R is Q_R , which follows the segment Q-R in the DE relaxation. The capacitance of the transducer reaches its maximum again along the path S-P, completing the rectangular conversion cycle P-Q-R-S-P.

$$E_{conv} = (V_{Max} - V_{Bias})(Q_s - Q_R) \quad (2)$$

3.1.1. Energy Conversion Circuits for DEGs

Several energy conversion circuits have been reported related to electrostatics energy conversion.^[100,101] However, the conversion unit proposed by Roundy et al. has been extensively used by researchers in the research area of DEGs.^[36,44] The prototype consists of a variable capacitive transducer (DEG) and two general-purpose diodes (D1, D2). The DEG is placed between the two diodes in the circuit, and with an applied offset voltage, the variable capacitor is biased. The primary purpose of the diodes in the circuit is to ensure electrical isolation and unidirectional current flow to the subsequent unit. **Figure 8a** shows the basic circuit for energy conversion using a DEG.^[36]

Analog electrical signals, resulting from DEG dynamics can be made applicable with rectification, filtration, and regulation. The subsequent sections critically review the state-of-the-art energy conversion units that enable maximum usable energy transfer to the load.^[102,103]

3.1.2. Self-Priming Circuit for Energy Conversion

A DEG is primed with a high-voltage direct current (DC) under both actuation and generation modes of operation, which can be

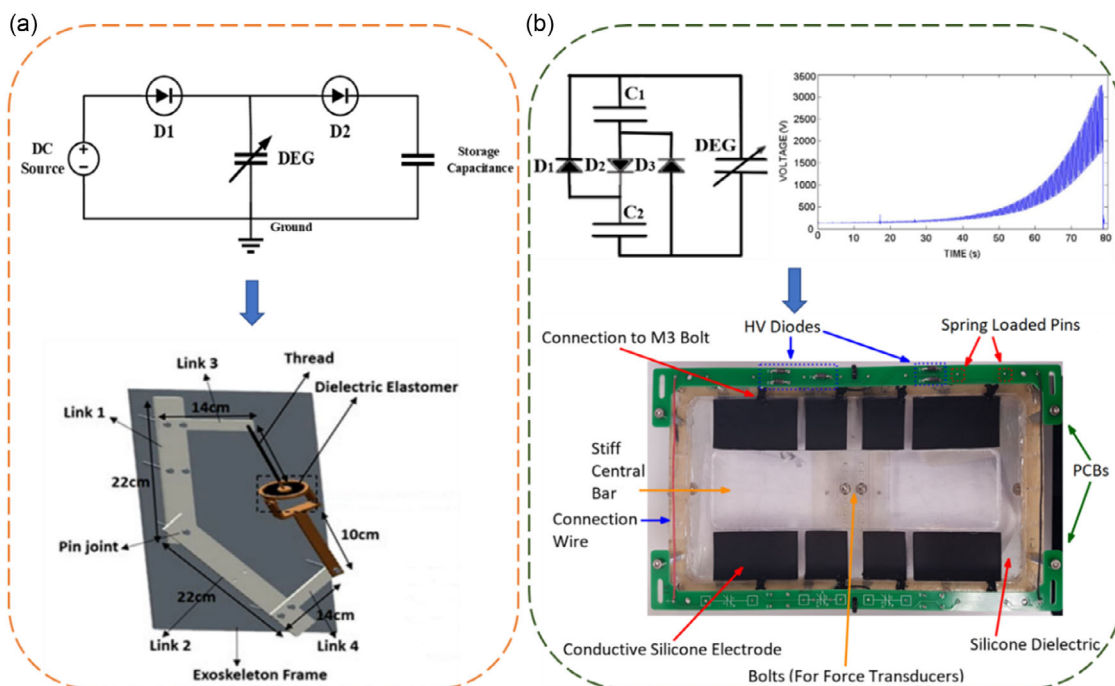


Figure 8. Circuits for energy conversion using DEGs. a) Primitive circuit diagram along with its utilization in a knee energy harvester.^[8] b) Dual stage self-priming circuit showing output voltage boosted from 10 to 3250 V using a DEG.^[111,233] along with the top view of self-priming circuit prototype.^[87,113]

a concern in applications such as wearable and standalone devices.^[104–108] Furthermore, the main challenge in developing an autonomous generation system using DEG is priming it with a high voltage.^[109] Therefore, a self-priming methodology was first introduced by McKay et al.^[110] which consists of a series and parallel configuration of passive components, such as diodes and capacitors. Figure 8b shows a self-priming methodology for a DEG. Later work by Ramanuja et al.^[111,112] adopted the concept of a self-priming circuit, which boosts the lower voltage DC passively by using discrete components. The self-priming circuit switches between two configurations where its capacitors are essentially in parallel (low voltage) and delivering charge to the stretched DE or in series (high voltage) for receipt of charge from the relaxed DE.^[113,114] Another self-filling DEG method was addressed and simulated by Shiju et al.^[115] where a part of a DEG output was used to prime the DE.

3.1.3. Interfacing Circuits for DEGs

The conditioning unit's primary goal is to synchronize the charge flow pumped by the periodical movement of the transducer connected to the DEG. An analog electrical signal that depends on the mechanical deformation of the DEG is produced when the deformed DEG pumps charge to the output terminal.^[116] However, the generated electrical signal needs to be processed to produce a usable output. Although the circuit explained in Figure 10 is widely adopted for energy conversion in laboratories, nonlinear switching of capacitances with material dynamics and the viscoelastic nature of the material can lead to certain

complications.^[91] Another major aspect of consideration is the use of a higher bias voltage (500–2000 V) to prime the DEG, which can make integrating the interfacing circuit difficult.^[117,118]

Since the development of DEGs, several electronics circuits have been discovered to interface. Over time, sophisticated developments in interfacing circuits have been reported.^[119] For example, Pelrine et al.^[120] explored the use of a potential divider circuit that could step down the output voltage to measure across the display unit. **Table 3** presents six types of interfacing units that have been reported by different researchers.

To generate electricity using a DEG, high-voltage biasing of a prestrained DE sample is essential. A potential divider circuit was first used to step down the generated output. However, the circuitual arrangement using a potential divider circuit profoundly affects the efficiency of the conversion system.^[121,122] To reduce the complexity and improve flexibility, some researchers have used high-voltage probes to stepdown the DEG output. However, this method is complex to implement for wearable and standalone devices. Subsequently, researchers used dynamic electronics switches as unidirectional and bidirectional power converters as interfacing units for DEGs. The following section explains the diverse interfacing circuits that have been reported and adopted by researchers.

3.1.4. Frequency-Dependent Interfacing Circuits

Depending on the nature of the input vibration, two different types of output patterns have been reported in **Figure 9**. The first

Table 3. Advancement of electronics related to DEGs.

Authors	Study	Findings
Due et al. ^[240]	The study provides a way to use DE as a transducer for harvesting mechanical energy at a lower frequency of vibration of DE	Proposed Buck/boost converter using two STP3N150 (1500 V) MOSFETs.
Peiwin et al. ^[103]	Prototype circuit for DEG under high-frequency vibration input (relatively small displacement of DE sample.)	The designed prototype was simulated using PSPICE. The prototype constitutes a low-pass filter followed by a switched-mode converter.
Wang et al. ^[102]	Forward path circuit for DEG with a distinct pattern of vibration	The electrical output of DEG was processed through a couple of stages: regulation and switched mode conversion. The circuit was operated in an open-loop condition.
Feng et al. ^[123]	A circuit prototype for dielectric polymer energy harvesting system	The study reveals a prototype that employs a transformer for boost and buck purposes simulated in MATLAB
Mass ^[241,242]	Driving the DEG with a multilevel high-voltage converter	Used multilevel boost converter to bias the DEG and used Buck converter to step down the voltage.
Zanini et al. ^[126]	Frequency-domain tradeoffs for DEGs Frequency-domain tradeoffs for DEGs	Compared the frequency-domain behavior of DEGs undergoing two different cycles, and different biasing voltages.
Ramanuja et al. ^[116]	Proposed an electrical model for a DEG	The proposed model and experimental investigations reveal a gain of 2.54 at DEG operating frequency of 2 Hz. Used fly-back converter to stepdown the voltage.
Anderson et al. ^[87]	Designed an autonomous electrostatic energy harvester with voltage-boosting	Self-priming circuit has been used for voltage boosting in DEG and a potential divider to measure output.
Sadangi et al. ^[243]	Energy conversion using donut-shaped DEG with relative analysis of stretch dependance capacitances	Controlled conditioning interfacing unit using MOSFET.

one is a low-frequency (1–2 Hz) signal damped on a primed DC voltage for high displacement of DE. The other is a high-frequency signal as high as 10 Hz which is expected for lower deformation of DE.^[103]

In sync with the generated signal pattern, the approach for interfacing circuits is classified into two different ways: low-frequency interfacing circuits and high-frequency interfacing circuits. However, in both circumstances, the resulting output voltage is high.^[123–125] Therefore, a stepdown circuit is desirable for a usable DC output.

For low-frequency circuits, researchers have focused on the higher displacement side of dielectric elastomers. The resulting output becomes an analog electrical signal with a low frequency and a high amplitude, which is analogous to that of the source. Several researchers have adapted diverse techniques for signal conditioning.^[44,102,103,123,124] Wang et al.^[124] presented a simulation of an interfacing unit for frequency-dependent DEG operation.

The interfacing circuits as in Figure 9 work on the principle of peak rectification and switching mode power conversion. Peak rectification is the first stage of the energy harvesting process. The process continues with a voltage regulator for a stabilized voltage level. The switched mode circuit acts as a step-down DC–DC converter.

In the case of the high-frequency circuit, the design has incorporated a low-pass filter followed by a DC–DC converter. This is because the maximum frequency signal for a DEG is considered to be 10 Hz. The low pass filtration technique assumes that the DE output signal is periodic.^[102,126] Figure 9 illustrates the impact of excitation frequency on the energy harvester's

conversion efficiency, with Mode 1 and Mode 2 representing sudden and gradual stretching of the membrane, respectively.

3.1.5. DEG Interfacing Circuits with Potential Divider and High Voltage Probes

Providing high voltage to DEG through a standalone supply is impractical, and hence a voltage booster is a crucial component for any DEG. To step down the converted electrical signal, Chiba et al.^[127] used a high-voltage probe at the DEG output terminal. Similarly, some researchers have adopted the potential divider method to quantify the generated analog signal.^[128] **Figure 10** shows a comprehensive review of both the methods of conversion that have been proposed and reported by researchers.^[103] The current has been made unidirectional from and to the DEG transducer using general-purpose diodes.

3.1.6. Interfacing Circuit for DEGs Using Dynamic Electronics Switch MOSFET

The use of a potential divider and high voltage probe for energy harvesting with a DEG has significant drawbacks due to high conduction losses caused by the associated resistances. To address this issue, several approaches have been proposed by researchers for better reduction of conduction losses.^[129] One such approach involves the use of a Zener diode and a dynamic electronic switch to reduce conduction losses with an increase in bias voltage.

Wang et al. proposed an interfacing circuit that consists of a diode, switched mode converter, and a regulator.^[103] The

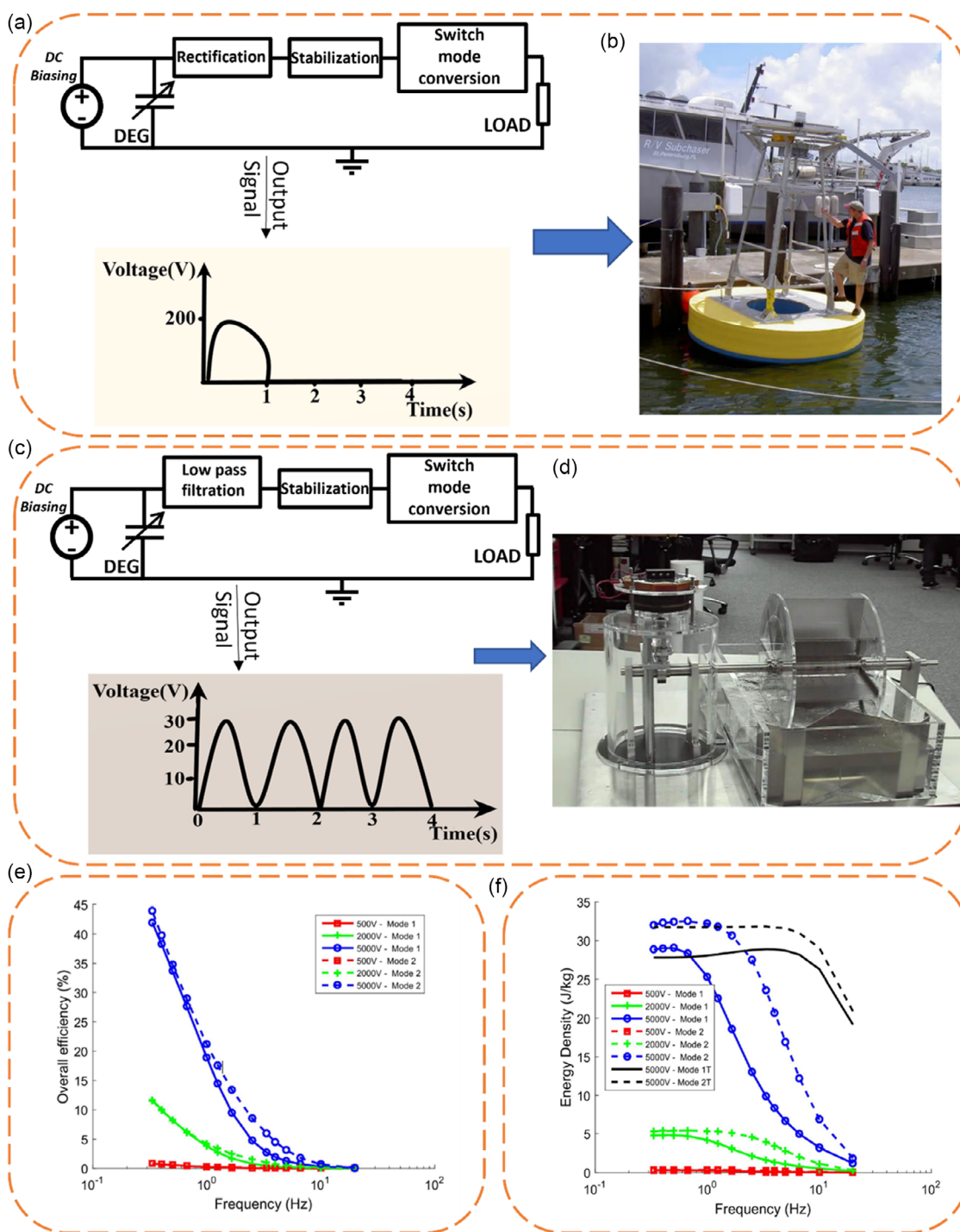


Figure 9. a) Circuit and output for low-frequency interfacing. b) Working prototype of a low-frequency input-based buoy-type wave energy harvester.^[2,102] c) Circuit and output for high-frequency interfacing. d) Working prototype of a high-frequency input-based water mill energy harvester.^[2,103] e,f) Effects of excitation frequency change on the conversion efficiency and energy density of an energy harvester.^[126]

conditioning circuit receives the electrical signal produced by the DEG, where the diode signifies unidirectional current flow. The regulator is responsible for regulating input voltage to a particular value, and the capacitor attached in parallel with the regulator acts as a passive filter to remove ripples at the output.

A MOSFET serves as the series component, and in the ideal scenario, the switch's power loss tends to be zero.

A dynamic electronic switch has been applied in two other circuit arrangements under their environment proposed by Mass et al.^[130] and further adopted by Panigrahi et al.^[131] The first

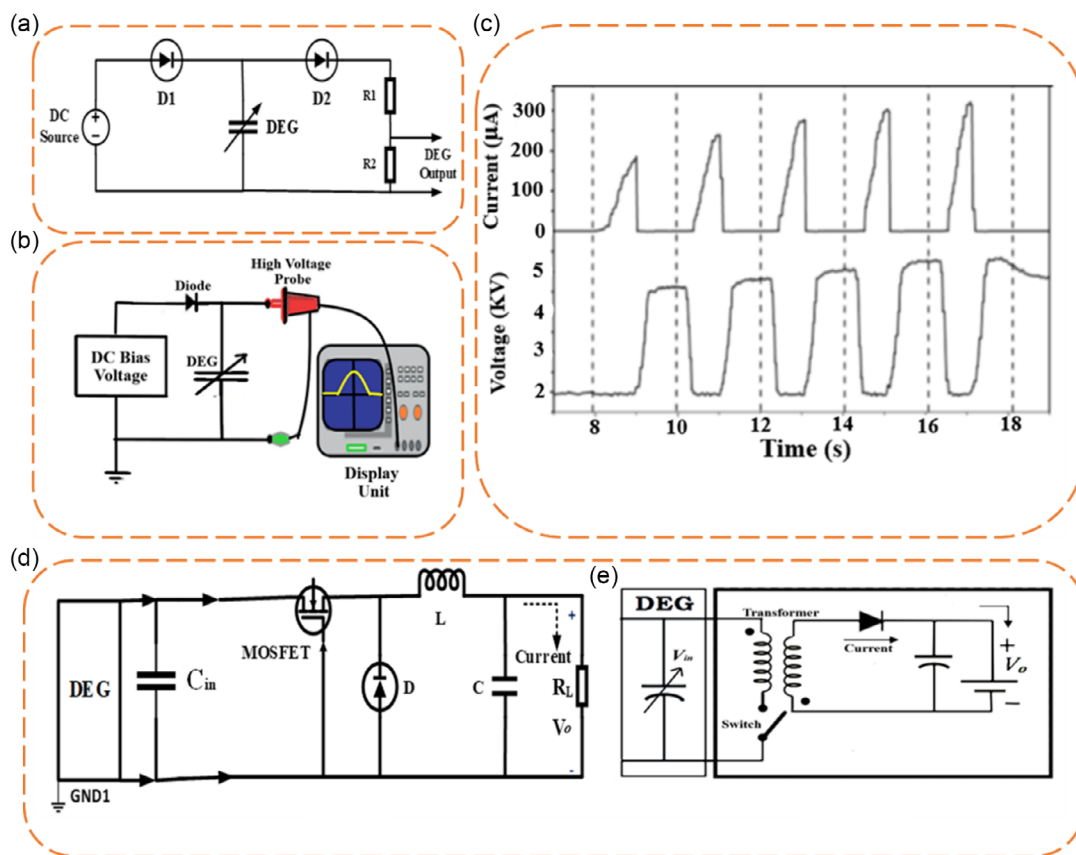


Figure 10. a) Circuit with a potential divider. b) DEG circuit with a high voltage probe. c) Output voltage and current correspond to a DEG deformation.^[103] d) Circuit with a buck converter using MOSFET.^[102] e) DEG circuit with a fly-back converter.^[116]

circuit is a bidirectional DC–DC converter that uses a series of MOSFETs as multiple switches for voltage boosting purposes, with a fly-back converter used at the output side of the DEG to handle small power outputs.^[132,133] The fly-back converter includes a low turn ratio transformer and uses a MOSFET as a dynamic switch at the secondary of the transformer. A diode connected in series with the secondary of the transformer ensures unidirectional current flow, while synchronous switching of the MOSFET with the DE deformation frequency enables maximum energy transfer.

4. Electromechanical Properties of DEGs

4.1. Mechanical Properties of DEGs for Energy Harvesting

In DEGs, the amount of energy that can be converted per unit cycle is predominantly influenced by the mechanical properties of the elastomers utilized.^[36,134] Therefore, it is imperative to conduct thorough investigations into the mechanical properties of DEs to ensure maximal utilization and enhanced performance of various DEGs. Moreover, it is noteworthy that the performance of DEGs is significantly impacted by the degree of pre-stretch applied to the DEs, particularly regarding their specific mode of operation and intended function.^[135] The mechanical

properties of DEs that have an impact on the performance of a DEG are outlined as follows.

4.1.1. Stiffness

Mechanical stiffness is a crucial factor for the operation of any DEGs as it determines the actuation load required for their functioning.^[136,137] A high stiffness can result in an increased actuation force, while a low stiffness can result in electromechanical instabilities in DEGs.^[138] **Figure 11** shows that materials such as natural rubber (Oppo Band) and styrene rubber (ZRU) have higher stiffness compared to acrylic rubber (VHB 4910). Therefore, it is essential to carefully consider the optimal stiffness of dielectric elastomers for efficient and stable DEG operation.

4.1.2. Stretchability

Dielectric elastomers possess an important mechanical property known as stretchability, which significantly influences the energy output of DEGs.^[59,139–142] Stretchability refers to the maximum mechanical stretch achievable during the cyclic operation of DEGs. This means that the higher the stretchability of the dielectric elastomer, the greater the energy output of the DEG,

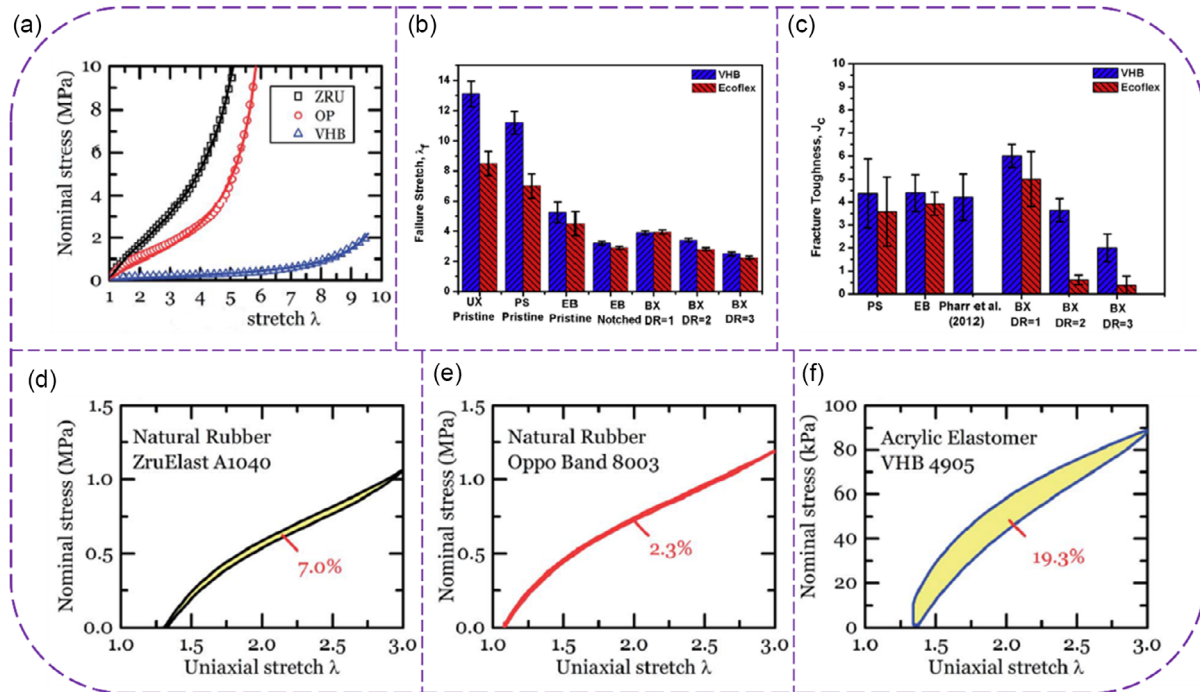


Figure 11. a) Stiffness comparison of three types of commercially available rubbers.^[234] b) Stretchability comparison of VHB and Ecoflex based on deformation modes.^[139] c) Fracture toughness comparison of VHB and Ecoflex for various deformation modes.^[139] d–f) Hysteresis behavior of commercially available dielectric elastomers.^[234]

highlighting its crucial role in optimizing DEG performance. In summary, the stretchability of dielectric elastomers is a foundational property that underpins the performance and applicability of DEGs, making it a vital area of research and development in the field of flexible electronics and energy conversion.

4.1.3. Viscoelastic Losses/hysteresis

The viscoelastic nature of elastomers results in significant hysteresis losses and stress relaxation, affecting the long-term behavior of DEGs. Hysteresis losses refer to the dissipative energy of a DE material during a loading-unloading cycle.^[143,144] Essentially, the stress induced during loading is higher than the stress induced during relaxation at a specific strain.^[88,100,145,146] This phenomenon is crucial when designing energy harvesting devices using DEs since they primarily deform in cyclic motion to generate energy.^[96,147] Previous studies have investigated hysteresis in DEs under uniaxial loading. For instance, Sahu et al.^[100] discovered that for VHB, increasing strain rates did not significantly increase hysteresis losses. In tests on silicone rubber, Rey et al.^[148] found that under a uniaxial force, the degree of hysteresis increased with temperature. Hysteresis of DEs typically correlates with both stretchability and fracture toughness. A higher hysteresis is indicative of greater fracture toughness and stretchability.^[144,149] Ahmad et al.^[139,150] investigated the effect of hysteresis losses in different modes of deformation, including uniaxial, pure shear, and equi-biaxial deformation, for VHB and Ecoflex, both used as DE materials. The research outcomes showed that the losses were consistently higher for VHB,

irrespective of the method of deformation. These findings underscore the critical nature of taking hysteresis into account when choosing dielectric elastomers for energy harvesting purposes, as it has the potential to greatly influence the performance of the device.

4.1.4. Fracture Toughness

The amount of energy required to prevent the initiation and propagation of a crack in a material is significantly influenced by its fracture toughness.^[141] In the case of DEGs, the primary cause of failure is the fracture of the materials, underscoring the critical importance of comprehending the fracture toughness of dielectric elastomers in the design of DEGs.^[151,152] An effective approach to enhance the durability and lifespan of DEGs involves the incorporation of materials with high fracture toughness.^[85,153] In addition to choosing materials with high fracture toughness, other methods to increase the toughness of dielectric elastomers include optimizing material processing techniques, developing filled elastomers, and implementing novel material designs like 3D printing. These approaches can further enhance the durability and performance of DEGs.

4.1.5. Flaw Sensitivity

The term flaw sensitivity pertains to the decrease in the ability of an elastomer to stretch as a result of imperfections and notches within the material.^[154,155] Flaws occur in the material during its production process, while notches may develop while the DEGs

are in operation. Understanding flaw sensitivity is crucial for the design of DEGs as it allows for the identification of operational limits and aids in the selection of suitable elastomers for long-term performance and durability.

4.2. Electric Properties Related to Energy Harvesting

It is crucial to thoroughly investigate the dielectric properties of DE materials, including their dielectric constant, dielectric breakdown strength, and dielectric loss. These properties significantly influence the performance of DEs when utilized in transducers or harvesters. As such, conducting a comprehensive examination of dielectric properties is essential to ensure their effective utilization and to optimize the performance of various DEGs.^[156–158] Additionally, analyzing the dielectric failure of DEs under different priming conditions and modes of deformation is essential for the proper understanding and functioning of DEGs.^[159] However, there is limited information on dielectric characterization techniques of DEs under multiaxial modes of deformation in the literature.^[160,161] Furthermore, to understand the effect of dielectric properties on the energy harvesting process, it is necessary to establish a relationship between various dielectric properties and the net amount of energy produced during the harvesting process.^[162,163]

$$U_o = \frac{1}{2} \times \epsilon_o \times \epsilon_r \times V \times E_{max}^2 \left[1 - \frac{A_{min}^2}{A_{max}^2} \right] \quad (3)$$

Equation (3) shows the harvested energy U_o is directly proportional to the dielectric constant ($\epsilon_o \times \epsilon_r$) and the volume V or mass m of a DEG. Furthermore, it is directly proportional to the square of the applied electric field (E_{max}^2). The harvested energy is directly related to the energy density of a dielectric elastomer material because only some of the energy stored inside the material can be converted for its use in applications (Figure 12).^[164,165]

4.2.1. Dielectric Constant

The dielectric constant, also known as relative permittivity, is a measure of the ability of a material to store electrical energy in an electrical field. It is expressed as the ratio of the permittivity of a material to that of a vacuum. A higher dielectric constant of an elastomer translates to a greater amount of electric energy that it can store or harvest. Therefore, for effective energy harvesting, a material with a high dielectric constant is crucial.^[166]

4.2.2. Dielectric Breakdown Strength

The dielectric breakdown strength is the amount of electric field that an elastomer can withstand without conducting electricity, even though it is an insulator material. The voltage at which the breakdown of elastomer occurs is known as the breakdown voltage. To withstand high bias voltage conditions, a dielectric elastomer material must have a high breakdown strength.

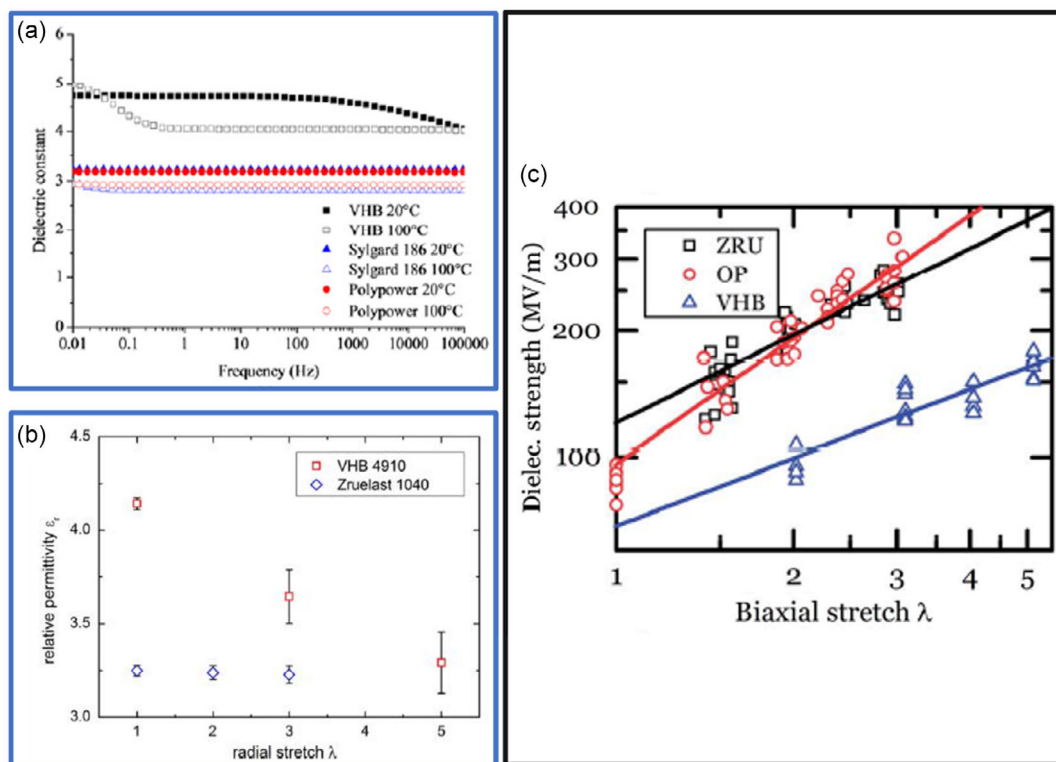


Figure 12. a,b) Dielectric constants of most commonly available acrylic and silicone rubbers at various frequencies and radial stretches.^[235,236] c) Variation in the dielectric strength with respect to increasing biaxial stretch for three different types of commercially available rubbers.^[234]

Table 4. Comparison of elastomers based on their electromechanical properties.

Properties	Natural rubber ^[11,150]	Acrylic ^[139,140,244]	Silicone ^[245–248]
Mechanical properties			
Shear modulus (stiffness) [kPa]	400–1000	20–70	300–850
Viscoelastic losses [%]	13–20	25–40	10–15
Stretchability	6–8	10–16	8–10
Fracture toughness [kJ m ⁻²]	7–9	4–6	2–4
Flaw sensitivity	Very low	Low	High
Electrical properties			
Dielectric constant	2.74	4.14	2.85
Dielectric breakdown strength [kV mm ⁻¹]	100–300	70–180	75–195
Conductivity [pS m ⁻¹]	0.1–0.4	1–5	0.0005–0.05
Energy density [J g ⁻¹]	0.16 mJ g	0.0625 mJ g	6.3 mJ g

This property is typically measured as the applied voltage per unit thickness of the DE material (Table 4).^[167–169]

4.3. Effects of DE Deformation Modes on DEG Performances

The deformation mechanism of a DE plays a critical role in maximizing energy conversion. The electrical energy stored in a DEG is directly proportional to its capacitance. Therefore, to increase the energy output of a DEG, it is imperative to maximize its capacitance change per cycle. This can be accomplished by actively controlling the deformation of the DEG, as capacitance is significantly influenced by the area and thickness of the DEG. Various deformation mechanisms have been identified for energy generation, including uniaxial, equal-biaxial, pure-shear (in-plane stretching), and conical and circularly inflated (out-plane stretching) deflections.^[170–175] The most commonly observed type of deformation is uniaxial, also known as simple extension. This occurs when the elastomer is stretched in one direction, while the lateral direction is free to contract.^[100,176] The sample length is typically assumed to be greater than or equal to 4–5 times the sample width.^[177] Even though using this prestretching technique is simpler, it can cause shrinking in the transverse direction, resulting in minimal capacitance change.

Pure shear is the second kind of deformation, in which a force is applied from one direction but the lateral side does not considerably contract.^[138,145] To ensure that lateral direction is tightly controlled in pure shear deformation, the width must be kept at least 10 times greater than the length. It provides a greater advantage of a higher active-to-passive area ratio, resulting in a large capacitance change and the prevention of loss in tension phenomenon.^[138,178] The most popular method of deformation is biaxial prestretching, which involves stretching an elastomer both longitudinally and laterally. Equi-biaxial deformation mode offers a greater benefit due to its simple prestretching ability and simplicity in holding the elastomer, which improves the functionality of DE transducers. In addition, the equi-biaxial deformation maximizes the capacitance variation achieved through

stretching in every direction. The applications of this mode of deformation are artificial muscles, pneumatic valves, disk drives, micro pumps, motors, etc.^[179,180] Koh et al.^[181] compared the in-plane modes of deformation and concluded that the equi-biaxial mode of deformation achieved the maximum energy density of 0.82 J g⁻¹.

A conical DEG model consists of an outer fixed circular ring with an elastomer sandwiched between its two halves and a movable hub at the center. This is somewhat similar to pure shear mode because the stretching is minimal in the circumferential direction.^[182–186] The structure is quite compatible to extract mechanical energy from the environment, but the energy density is one order lower than equi-biaxial stretching.^[36,187] A circular inflated DEG model also consists of an outer fixed hub with an elastomer sandwiched between its two halves. It utilizes the pressure difference between the inside and the outside of a DEG for stretching. This mode of deformation is quite similar to equi-biaxial stretching but its energy density is slightly lower due to the strain energy density being dependent on the amount of membrane deflection.^[39] Figure 13 shows uniaxial, equi-biaxial, conical, pure shear, and circular inflated modes of deformation. Few studies exist in the literature on the comparison of these deformation modes and their effects on energy harvesting performance. Table 5 shows a comparison of various deformation modes based on their harvesting performance, and it is evident that the equi-biaxial deformation mode has the highest energy density compared to others because it can achieve a large amount of stretching in a given electrode surface area.^[188]

4.4. Effects of Environmental Factors on Failure Modes of Dielectric Elastomers

Environmental conditions, such as temperature and humidity, significantly impact the energy generation performance of DE materials. Temperature, in particular, plays a critical role in influencing the mechanical and electrical behavior of these elastomers. Under typical conditions, an increase in ambient temperature enhances the stretchability of the elastomer due to thermal expansion, while also increasing viscoelastic losses, which can negatively affect efficiency. Additionally, higher temperatures tend to reduce the dielectric constant of the material, as the thermal field causes rearrangement of dipoles within the elastomer matrix.

Chen et al.^[189] explored the influence of temperature on the performance of DEGs, focusing on failure modes such as loss of tension and electromechanical instability. His findings revealed that the critical electric field required to trigger these failure modes increases with temperature. This occurs because elevated temperatures promote inelastic stretch within the elastomer, increasing its capacity to withstand higher electric fields before mechanical failure ensues. As a result, dielectric elastomers can sustain more deformation at higher temperatures, albeit at the cost of additional energy loss due to viscoelastic dissipation. In another study, Bele et al.^[190] examined the effects of temperature and humidity on the electrical breakdown field of silicone-based dielectric elastomer films. Their results showed that temperature had a measurable influence on the breakdown field, which slightly increased as the temperature rose. This was

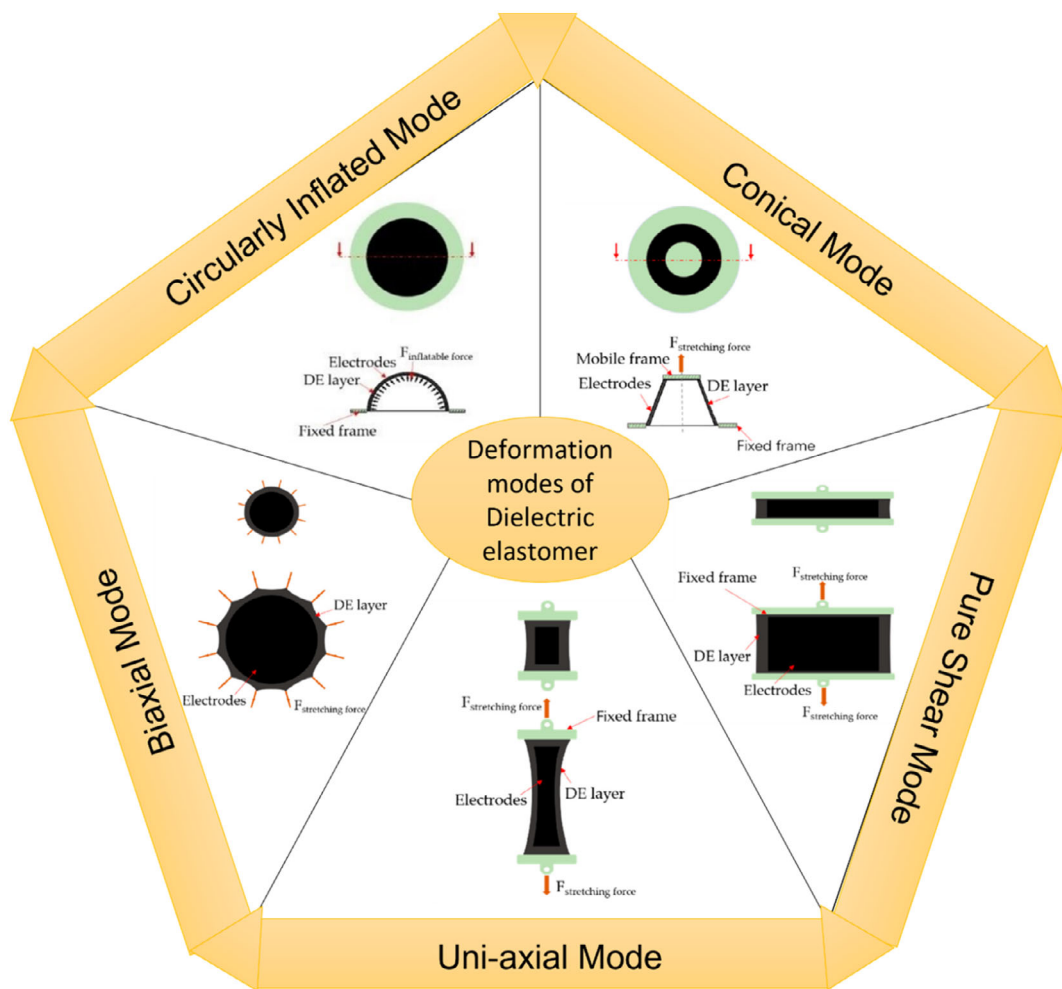


Figure 13. Deformation modes of various DEG prototypes.^[39]

attributed to enhanced mobility and rearrangement of dipoles within the silicone polymer chains, leading to a more stable configuration under the applied electric field. Interestingly, they found that humidity had a negligible effect on the electrical breakdown threshold of silicone elastomers. However, humidity significantly influenced the viscoelastic behavior of the material, particularly its dynamic viscoelastic creep.

Zuo et al.^[191] further investigated the impact of humidity on dielectric elastomers and reported that dynamic viscoelastic

Table 5. Existing DEG deformation modes and their respective energy harvesting performances.

Deformation mode	Energy output [mJ g]	Efficiency [%]
Equi-biaxial ^[237]	780	30
Circular diaphragm ^[134]	145	18
Uniaxial ^[249]	78.4	17.19
Conical stretching ^[127]	46.58	12
Pure shear ^[73]	2.88	3.8

creep is highly sensitive to changes in humidity. They observed that increasing the relative humidity from 20% to 80% resulted in a dramatic 1600% rise in the equilibrium position of dynamic viscoelastic creep for samples prestretched to a ratio of 3, as illustrated in **Figure 14**. This suggests that while humidity may not directly affect the electrical failure modes of the elastomer, it greatly alters its mechanical behavior over time, particularly in applications where long-term cyclic actuation is required.

Overall, the interplay between temperature and humidity must be carefully considered when designing and optimizing dielectric elastomer systems for energy generation and actuation, as these environmental factors can have profound effects on both electrical stability and mechanical performance.

4.5. Long-Term Performance of Dielectric Elastomers

The long-term performance, or durability, of DEs is a critical factor determining their feasibility for real-world applications. Durability in dielectric elastomers depends on a range of parameters, including mechanical stretch ratios, bias voltage, and

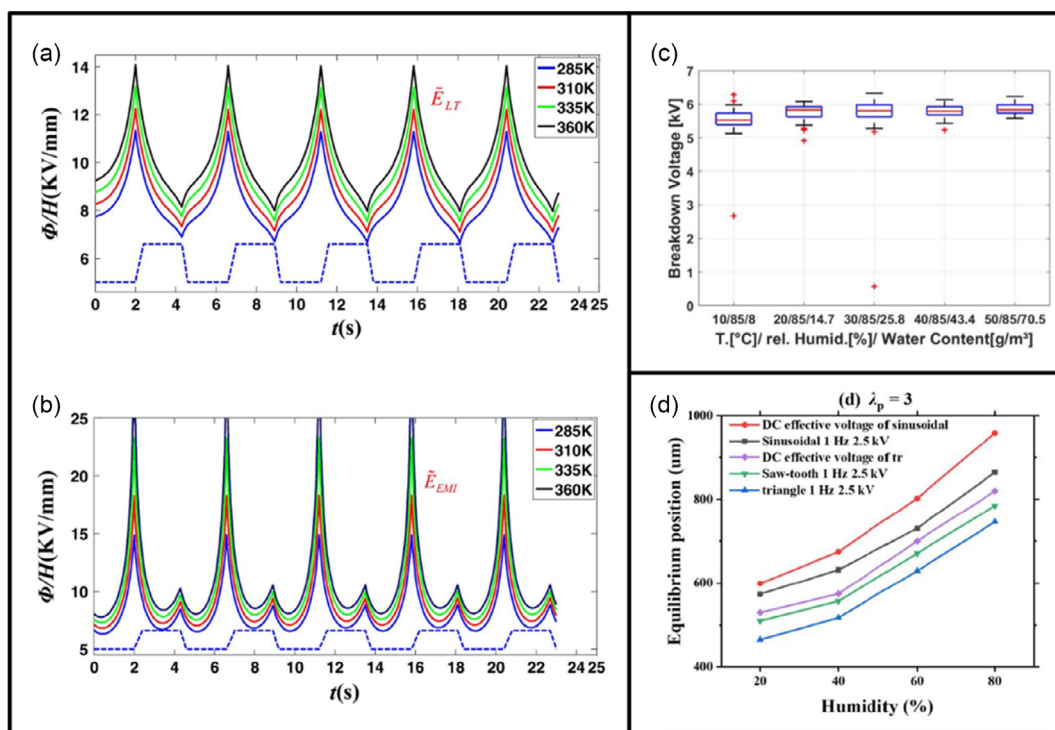


Figure 14. a) The critical condition of loss of tension under different operating temperatures.^[189] b) The critical condition of electromechanical instability under different operating temperatures.^[189] c) Influence of temperature on breakdown voltage @constant relative humidity.^[190] d) The equilibrium position of VHB 4905 under the prestretch ratio of 3 and different voltage waveforms.^[191]

electric breakdown strength. In particular, DEs are subjected to multiple failure modes, such as electric breakdown, rupture, and loss of tension, which can significantly limit their operational lifespan.

4.5.1. Electric Breakdown and Mechanical Stretching

One of the primary failure mechanisms affecting the longevity of dielectric elastomers is the electric breakdown limit. This phenomenon occurs when the applied electric field exceeds the material's capacity to withstand voltage, causing dielectric failure. Xu et al.^[192] conducted a detailed study on how mechanical stretching impacts the electric breakdown strength of DEs, given that electric breakdown is one of the main determinants of a dielectric elastomer's lifespan. His findings revealed a complex relationship between mechanical strain and electric breakdown.

On one hand, the study demonstrated that increasing mechanical strain (stretch ratio) enhances the breakdown voltage, meaning the material can sustain a higher electric field before breakdown occurs. This is because stretching causes the elastomer to thin, thereby requiring a higher voltage to generate the same electric field strength, as shown in **Figure 15a**. However, Xu also noted that stretching the material can amplify the presence of microscopic defects or impurities within the elastomer, such as air pockets, particles, or material inhomogeneities. These imperfections act as stress concentrators and result in localized regions of elevated electric field, which drastically lower the overall breakdown strength. Consequently, excessive stretching

beyond a critical limit can lead to premature failure, despite the initial increase in breakdown voltage. Therefore, when designing dielectric elastomer systems, mechanical strain should be optimized and kept below the rupture limit to maximize both the breakdown strength and durability of the material.

4.5.2. Fatigue Life and Electrode Compliance

Another key factor influencing the long-term performance of dielectric elastomers is fatigue life, which refers to the material's ability to endure repeated cycles of mechanical and electrical loading without failure. Fatigue life is particularly important for applications like DEGs, where the material undergoes continuous actuation. Yao et al.^[85] demonstrated that improving the compliance between the dielectric elastomer and the flexible electrode materials can significantly enhance the fatigue resistance and longevity of the system.

In their study, Yao et al. used silicone rubber as the base dielectric elastomer, combined with flexible electrodes made out of a mixture of silicone rubber (100 phr) with CG (40 phr) and CB (5 phr) and vulcanizing agent tetraethyl orthosilicate (5, 10, and 20 wt% of uncured silicone rubber) named SRE-1, SRE-2, and SRE-3, respectively, based on the amount of vulcanizing agent presence. This combination reduced the fractional resistance at the interface between the dielectric elastomer and the electrode, allowing for smoother electrical conduction and minimizing localized stress concentrations at the interface. This improved electrical and mechanical coupling was found to

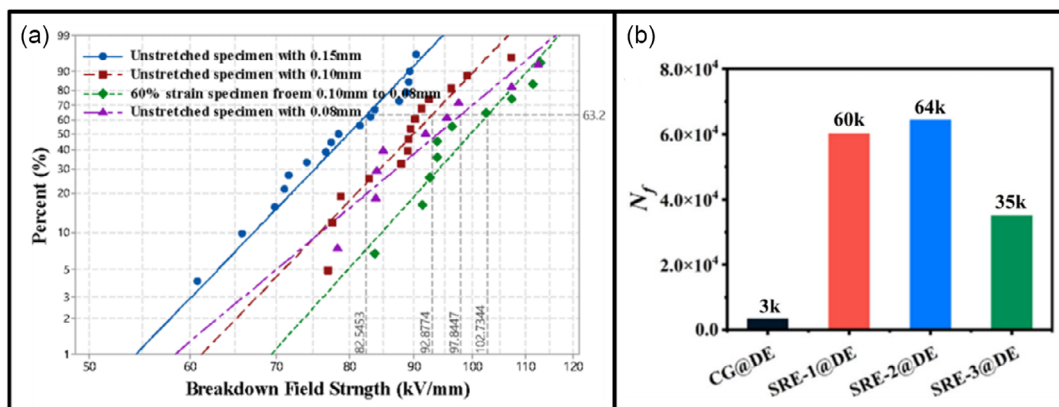


Figure 15. a) Weibull distribution of material breakdown field strength for PDMS specimens.^[192] b) Fatigue life of different combinations of elastomer film with silicone rubber-based flexible electrodes.^[85]

extend the fatigue life of the dielectric elastomer by 20.3 times compared to traditional electrode materials, as shown in Figure 15b. By maintaining a uniform distribution of electric charge and avoiding mechanical degradation at the elastomer-electrode interface, the overall system was able to sustain long-term cyclic actuation without significant performance losses.

4.5.3. Other Factors Affecting Durability

In addition to electric breakdown and fatigue life, the durability of dielectric elastomers is influenced by several other factors: 1) Loss of Tension: Over time, repeated cyclic loading can lead to a gradual loss of tension in the elastomer, affecting its ability to return to its original shape. This loss of tension, combined with viscoelastic creep, reduces the efficiency of energy generation and actuation in DEs over extended periods; 2) Environmental Conditions: As discussed in earlier sections, factors such as temperature and humidity also have a considerable impact on the long-term performance of dielectric elastomers. Elevated temperatures can enhance stretchability and increase viscoelastic losses, while humidity affects viscoelastic creep, altering the mechanical properties of the material over time; 3) Mechanical Prestretch: Mechanical prestretching is often used to improve the performance of dielectric elastomers, increasing their ability to sustain high electric fields. However, excessive prestretching can lead to material fatigue and eventual rupture if not carefully managed. Optimizing the prestretch ratio is crucial for maximizing the elastomer's lifespan without compromising performance; and 4) Material Composition and Aging: The inherent properties of the dielectric elastomer material, including its chemical composition and molecular structure, play a fundamental role in determining its long-term durability. Aging effects, such as polymer chain degradation or oxidation, can gradually reduce the elastomer's mechanical strength and dielectric properties, limiting its operational lifespan. Developing elastomers with enhanced aging resistance or adding stabilizers to delay material degradation can help extend the long-term usability of these materials.

4.5.4. Strategies to Enhance Durability

To improve the long-term performance and durability of dielectric elastomers, researchers and engineers have explored several approaches, including: 1) Material Innovations: Developing new dielectric elastomer formulations with higher dielectric breakdown strength and better fatigue resistance, such as using advanced silicone-based elastomers or incorporating nanocomposites to improve mechanical strength and electrical properties; 2) Enhanced Electrode Design: Using flexible, conductive materials like carbon nanotubes, graphene, or metallic nanowires as compliant electrodes can reduce interfacial resistance and increase the fatigue life of DEs; and 3) Protective Coatings: Applying thin protective coatings to the surface of the dielectric elastomer can help prevent mechanical degradation and environmental damage, thus extending the material's operational life.

In conclusion, the long-term performance of dielectric elastomers depends on a delicate balance between mechanical, electrical, and environmental factors. Optimizing these parameters, along with improvements in material design and system configuration, can significantly enhance the durability and reliability of dielectric elastomers, making them more suitable for demanding applications in energy generation and soft robotics.

5. DEG Prototypes and their Performances

Nowadays, a lot of scientific research is focused on harvesting renewable energy. As mentioned in previous sections, DEG's high energy density, electromechanical conversion efficiency, and high deformability have demonstrated its potential for energy harvesting. Theoretical energy density for dielectric elastomers lies within the range of $0.06\text{--}2.5\text{ J cm}^{-3}$ (i.e., $0.04\text{--}2.4\text{ J g}^{-1}$, as density of elastomers lies within the range of $0.96\text{--}1\text{ g cm}^{-3}$) presuming that the range of 200–500% is the maximum–minimum stretch ratio for equi-biaxial deformation.^[193,194] This value is three times greater than piezoelectric harvesters' energy density^[195,196] and the energy density of electrostrictive polymers^[197] by 10–100 times, which are capable of much lower strains. We will review research on the use of DEG

in the harvesting of renewable energy sources in this section, which includes human motion, wind, and waves. Since human motion energy-based DEGs typically generate power in the microwatt range, they are best suited for a variety of wearable devices, such as body implants, fitness bands, and biosensors. However, the power produced by wind and wave DEGs is at the kilowatt level, which is adequate to power coastal homes and structures as well as offshore buoys (Figure 16).

5.1. Prototypes Based on Energy Harvesting from Human Motion

The use of wearable devices, such as fitness bands, wireless earphones, miniature heart rate monitors, smart glasses, smart clothes, body implants, and various other devices to monitor the physiological activity of the human body, is rapidly increasing. These devices require a very low power to operate, typically in the range of a few microwatts. Such an amount of energy can be feasibly generated by various motions of body parts like walking, running, jumping, hand gestures, cycling, yoga, and various exercises.^[36,198,199] For example, during running at a frequency of 1 Hz (two steps per second), heel strike generates $\approx 2\text{--}20\text{ W}$ of power. Knee motion generates 35 W during deceleration with the help of muscles, while the center of mass movement of the body during jumping generates 20 W of power.^[200]

A heel strike generator was created by Kornbluh et al. that used striking of the heel to inflate a circular membrane of VHB 4910 with a maximum energy density of 0.3 J g^{-1} .^[31] It is estimated that this device is capable of generating 0.8 J or 1 W of power per step while walking.^[31] The prototype figure is shown in Figure 17a. Anderson et al.^[24] also developed a heel strike generator, which uses stacks of acrylic elastomer situated just below the heel, as shown in Figure 17b. Three stacks of elastomers, each of them containing 20 layers are placed in the heel section of the shoe, generating $\approx 30\text{--}40\text{ mW}$ of power within only 1 cm^2 of area.

Lagomarsini et al.^[10] developed a DEG with piezoelectric material as a priming source, as shown in Figure 17c. This prototype harvests $17.13\text{ }\mu\text{J}$ of energy per cycle of knee articulation motion. A kneepad-integrated DEG that can capture $112\text{ }\mu\text{J}$ energy at 1 Hz was created by Jean et al.^[201] A modified

commercial knee brace created by Slade et al.^[198] captures energy when the wearer is walking, and $3.13\text{ }\mu\text{W}$ of average output power can be generated. The figures of these knee pad harvesters are shown in Figure 17d,e. Sahu et al.^[8] developed a knee bending generator with a dielectric elastomer deforming in a conical fashion, as shown in Figure 17f. This prototype harvests maximum specific energy of 7.26 mJ g^{-1} with 25% of conversion efficiency at 1 Hz of excitation frequency.

Xie et al.^[202,203] in 2024, developed a combination of an electret nanogenerator (ENG) with an alternate current-based dielectric elastomer generator (AC-DEG), as shown in Figure 17g. The elastomer membrane does not require external voltage for biasing as the hydrogel-based nanogenerator sandwiched between the elastomer layers supplies the alternative current-based bias voltage. This prototype generated 3.214 mW of power with very small plane-strain of 44%.

5.2. Prototypes Based on Energy Harvesting from Wave Energy

WEC technologies have struggled to become commercially viable despite extensive research and development efforts targeted at creating devices that can harness the energy of ocean waves.^[204] The primary reason for this is the incapacity of mechanical and electromagnetic generating technologies to meet the requirements of the marine environment. Therefore, the potential use of DE materials has triggered a paradigm shift for radically new WEC technologies.^[205] DE materials offer unique benefits relating to the marine environment such as a lower mass density for easier deployment and maintenance, corrosion resistance, and a flexible nature that enables a high operational bandwidth.^[38,206,207] These attributes culminate in lower operating (OPEX) and capital expenditure (CAPEX); a crucial aspect of renewable energy technologies, which in turn calculates the levelized cost of energy (LCOE).

There have been several proposed DEG-based WECs to date, which can be implemented in two approaches: distributed generation and point power generation, depending on the device dimensions relative to the sea wavelengths (typically around 102 m).^[2,4,6,14,208–210] Point power generators are much smaller ($<5\text{ m}$) than the sea wavelength, while distributed generators have dimensions closer to the sea wavelength

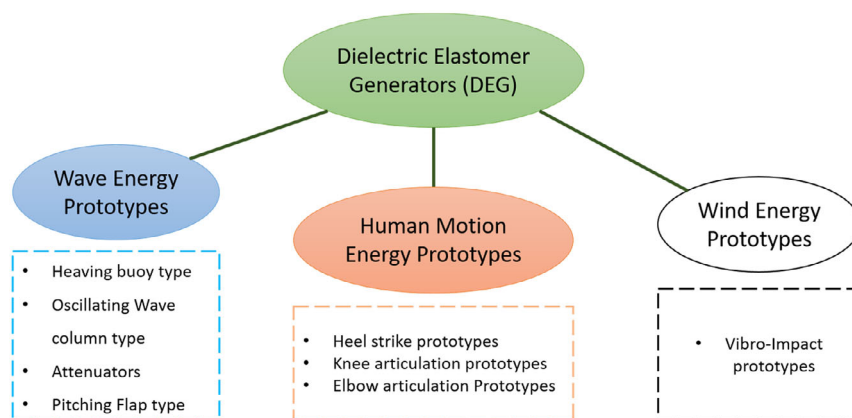


Figure 16. Different types of DEG prototypes available for harvesting ambient renewable energy into electrical energy.

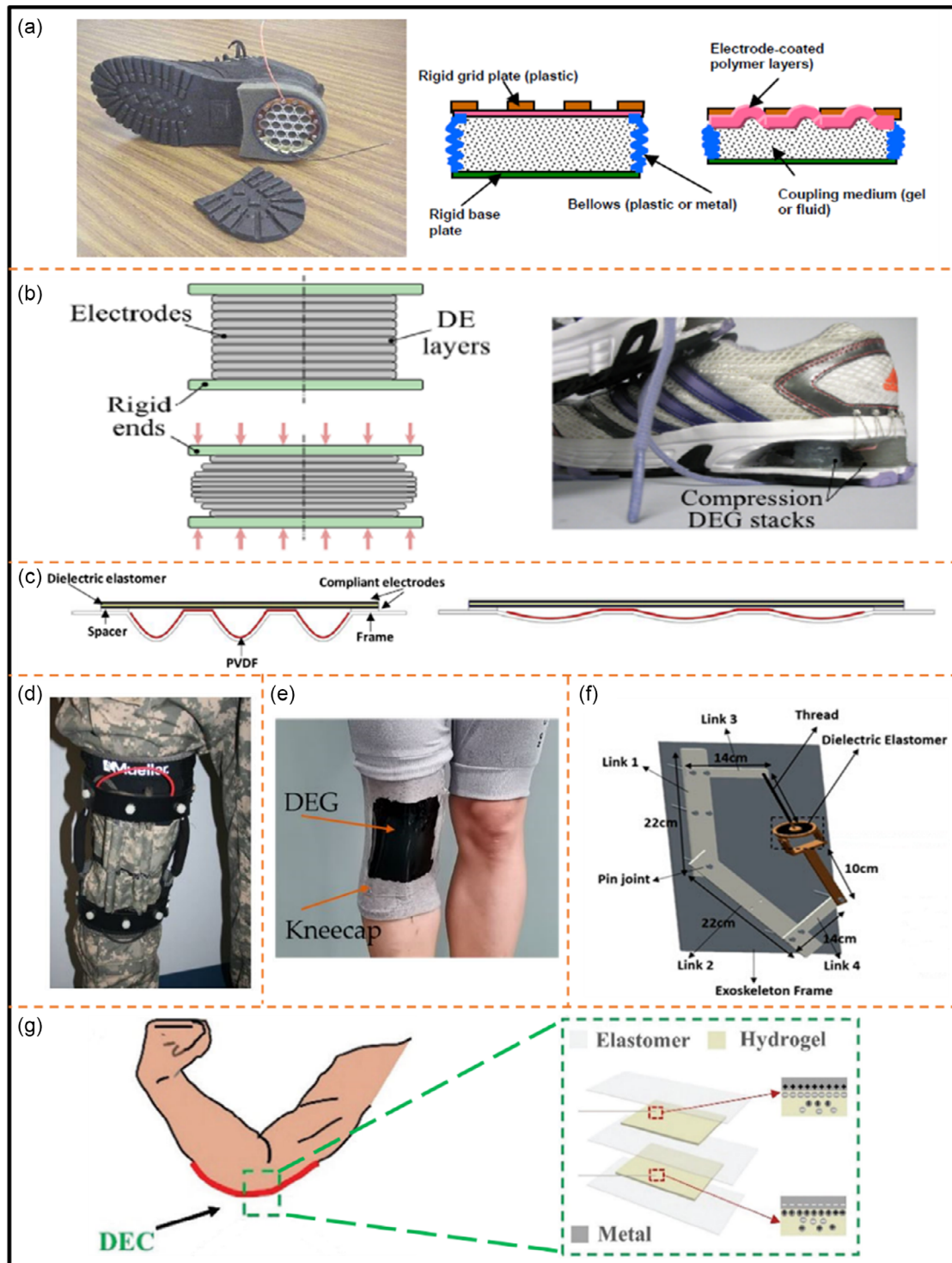


Figure 17. DEGs harvest energy from human motions. a) Picture and schematic of heel strike generator with an inflatable acrylic elastomer membrane developed by Kornbluth et al.^[31,36] b) Schematic and picture of a stack-based heel strike generator developed by Anderson et al.^[24,36] c) Schematic of a DEG with PVDF piezo-polymer as priming source and using knee articulation, developed by Logomarsini et al.^[10,36] d) Kneepad articulated generator developed for army cadets.^[201] e) Wearable kneepad strip for energy harvesting from knee articulation.^[198] f) Schematic of a knee-attaching exoskeleton for energy harvesting via conical deformation of elastomer membrane.^[8] g) Schematic of elbow articulation-based hybrid DEG which utilizes ENG sandwiched b/w the elastomer layer for self-biasing.^[202,203]

(<100 m),^[211,212] DE-based point absorber WECs are most extensively studied so far since the existing electromagnetic generator power take-off (PTO) can be easily replaced with a DEG PTO.^[31,213,214] These devices comprise a primary hydrodynamic interface that interacts with waves to serve as a buffer for potential and kinetic energy. The conversion of mechanical energy into electrical power is handled by the DEG PTO system.^[215] A floating buoy (e.g., a pitching flap^[213] or a heaving buoy^[216]) or an amount of seawater channeled into a vertical column, known as an oscillating water column (OWC)^[214,217–219] can be utilized as primary interface. The wave loads oscillate the interface, which propels the DEG PTO's cyclical deformation.

Hyper Drive Corporation (Japan) and Stanford Research Institute (USA) proposed and demonstrated the first DE-based point absorber WEC.^[2,31] In 2005, a small-scale floating buoy demonstration using DEG PTO was built, and it was tested in the ocean. The system consisted of a tube of DEG (DE acrylic polymer weighted 300 g, 0.3 m in diameter), which was attached to a floating barge and a proof mass through the other end. An

output of 0.25 W on average, with 1.2 W at its highest points, was obtained during tests in moderate sea conditions. However, the authors assert that by using a greater priming voltage, a power output of up to 11 W could have been achieved.^[37] The prototype is shown in **Figure 18**.

Two fully functional OWC-type WEC prototypes were studied with help of an in house wave generator with 40 or 30:1 scale, as shown in Figure 18.^[134,220] In the first test,^[134] with DE material weighing 4.4 g, power outputs of up to 0.87 W and up to 18% wave energy to electrical energy conversion efficiency were achieved. In another test,^[221] up to 3.8 W of power output was achieved utilizing larger DEG samples (DE material weighing 19.5 g). These powers correspond roughly to outputs of 300–600 kW at full size, according to dynamic scaling laws.

SBM Offshore presented the S3, a tubular structure with two ends that are sealed off and loaded with water under high pressure.^[222] The structure is made up of DEGs that are formed into tubular segments by rolling electrode-coated DE membranes, as shown in Figure 18. These tubular structure of DE material are

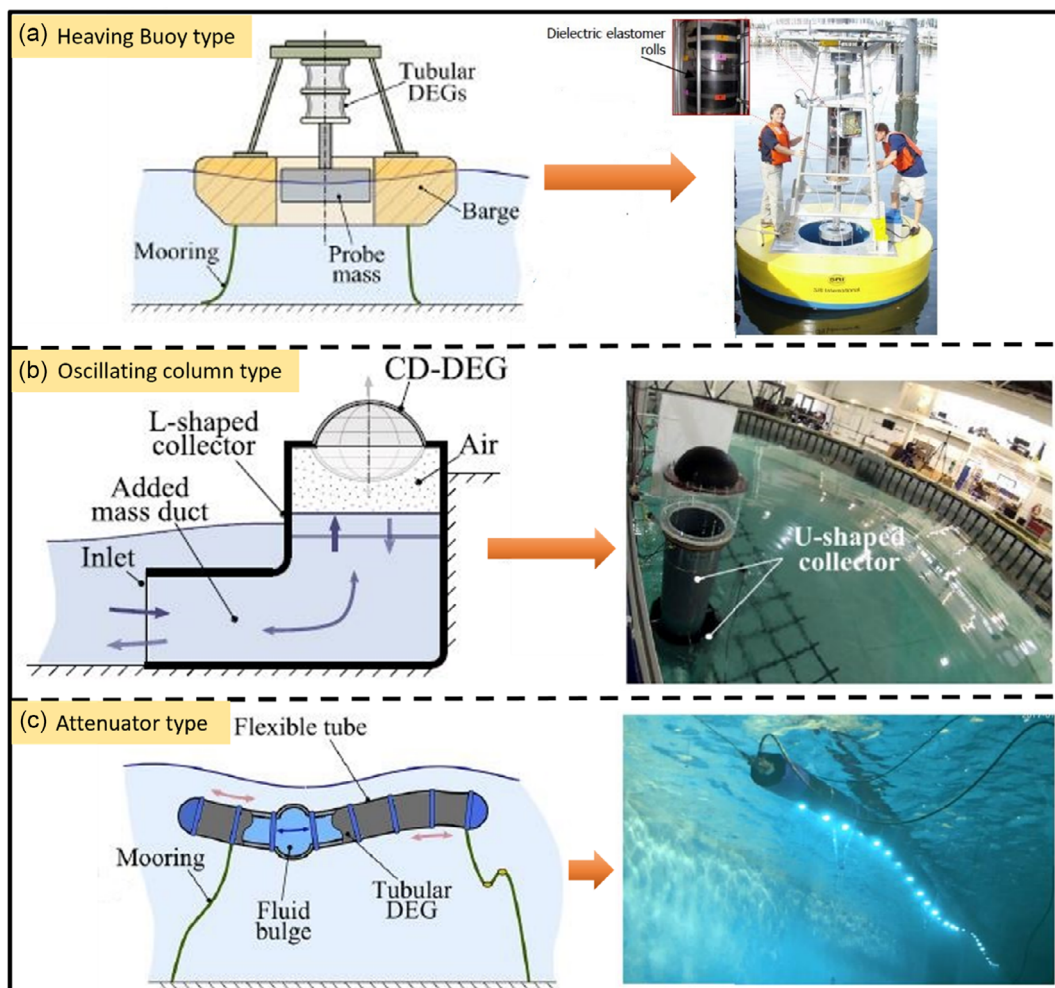


Figure 18. a) Sketch and prototype of a tubular DEG PTO-equipped heaving buoy-type WEC used by Chiba et al.^[36,37] b) Sketch and prototype of an OWC type WEC with a circular diaphragm type DEG PTO, investigated by Veretchy et al.^[36,134] c) Sketch and prototype image of a bulge shaped attenuator submerged in the sea, deployed by Jean et al.^[36,222]

prestretched due to pressurized water. Because the WEC length is similar to average sea wavelengths, individual sections will experience varied hydrodynamic pressures, which will lead to localized radial expansions of the various segments. The authors suggest that substantially more power production is possible if bigger electric fields (still below the breakdown limit) had been used, even though the actual peak electrical power they were able to produce was just 2 W.

In 2022, Du et al. suggested a unique OWC-type wave energy-based DEG system with a supplementary wind turbine generator supplying self-bias voltage.^[4] With a bias voltage of 1.0 kV and a deformation displacement of 120 mm applied to the DE film, the maximum electrical energy converted is around 1.4 J.

5.3. Prototypes Based on Energy Harvesting from Wind Energy

The last couple of years have witnessed success in the field of renewable energy for the transformation of wind power into electrical energy, due to a lower LCOE that makes it a desirable prospect.

In 2017, Yurchenko et al.^[223] proposed the vibro-impact (VI) DEG system which can harvest vibration energy from the environment. Subsequently, many researchers further investigated VI-DEGs.^[165,224–226] Based on this principle, Zhang et al.^[20] created a device to be used in wind energy collection, as shown

in **Figure 19a,b**. Through numerical simulations, the author investigated the VI-DEG's effectiveness at capturing wind energy.^[20] Results suggested that wind speed has a substantial impact on the VI-DEG energy collection system's performance. However, no experiments have been performed to support these findings.

Lai et al.^[227] conducted a study on another VI-DEG-based wind energy harvester. As depicted in Figure 19c,d, the DEG is incorporated into a cuboid bluff structure, which propels the VI-DEG in the direction of the wind. Using numerical models, the system's electrical and dynamic outputs under various wind speeds were examined. However, prior numerical studies have demonstrated that the DEG is limited to gathering wind energy within a particular wind speed range, indicating the need for further innovations in the structural design to fully utilize DEG's potential for wind energy harvesting (**Table 6**).

6. Challenge and Future Prospects

DEGs hold considerable promise for energy harvesting from ambient sources. However, to fully realize their potential, several significant challenges need to be addressed. Additionally, exploring future research directions will be crucial for advancing DEG technology. The detailed discussion of the challenges and future prospects for DEGs is as follows.

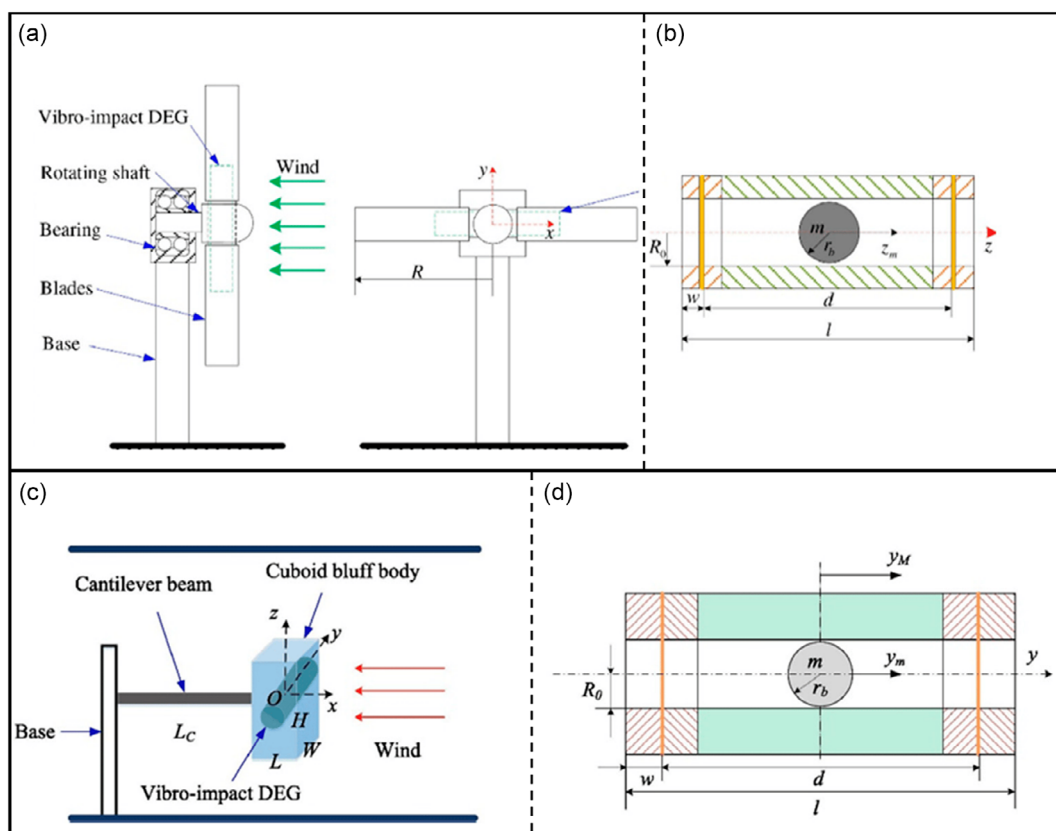


Figure 19. a) Schematic of a vibro-impact type wind energy harvester. b) Internal structure of a vibro-impact type wind energy harvester.^[223] c) Diagram of a rotating cuboid bluff body type wind energy harvester. d) Internal structure of a rotating cuboid bluff body type wind energy harvester.^[227]

Table 6. Energy harvesting comparison of various DE-based generator prototypes.

Application type	Harvester specification	Material used	Topology	Energy output	Power output	Efficiency [%]
Human motion	Heel strike ^[31]	VHB 4910 (20 stacked layers)	Circular diaphragm	0.3 J g	1 W per step	33
	Heel strike ^[24]	VHB 4910 (20 stacked layers)	Equi-biaxial	0.012 J g	30–40 mW per step	3.5
	Knee articulation ^[10]	VHB 4910 + PZT/PVDF	Pure shear	14.3 $\mu\text{J g}^{-1}$	21.4 μW per knee articulation	9
	Knee articulation ^[198]	VHB 4910	Equi-biaxial	13.3 $\mu\text{J g}^{-1}$	140 μW at 200 V	60
	Knee articulation ^[8]	VHB 4910	Conical stretching	7.26 mJ g ⁻¹	19.6 mW at 1500 V	25
	Elbow articulation ^[202]	VHB 4910	Equi-biaxial	–	3.215 mW at 1200 V	13
Wave energy	Heaving Buoy ^[2]	VHB 4910	Conical stretching	40 J g ⁻¹	11 W per cycle	20
	Oscillating wave column ^[134]	VHB 4910	Circular diaphragm	0.2 J g ⁻¹	3.8 W per cycle	18
	Oscillating wave column ^[4]	VHB4910	Circular diaphragm	1.4 J g ⁻¹	1.75 W per cycle	16
	Bulge wave attenuator ^[222]	Silicone elastomer	Pure shear	–	2 W per cycle	10
Wind energy	Vibro_Impact type ^[223]	VHB 4910	Circular diaphragm	3.2 mJ g ⁻¹	0.132 mW per cycle	5
	Cuboid Bluff body type ^[227]	VHB 4910	Circular diaphragm	1.5 mJ g ⁻¹	0.16 W per cycle	7

6.1. Challenges

6.1.1. Durability and Lifetime

The longevity of dielectric elastomers in energy harvesting applications remains a critical issue. DEGs are subjected to repeated mechanical stretching and electrical stress, leading to potential degradation over time. Current research has not adequately addressed the combined effects of mechanical fatigue and dielectric breakdown fatigue. To improve durability, there is a need for the development of novel elastomer materials that can withstand long-term operational stresses. Silicone-based materials have shown promise due to their flexibility and stability, but further research is needed to enhance their resistance to mechanical wear and electrical breakdown. Innovations in material formulation, such as incorporating advanced crosslinking agents or hybrid composites, could significantly extend the lifespan of DEGs and enhance their reliability for practical applications.

6.1.2. Scale-up

Achieving kilowatt-scale energy output with DEGs involves significant technical challenges. Scaling up from laboratory prototypes to large-scale systems requires advancements in the production of multilayer dielectric-electrode structures and thin-film dielectric membranes. The development of high-power bidirectional direct current electronics is essential for effective energy storage and management. Additionally, modular designs that allow for easy maintenance, control, and replacement of DEG components are crucial for large-scale deployment. Addressing these issues involves developing scalable manufacturing techniques, optimizing the integration of DEG systems with power electronics, and creating robust modular frameworks to facilitate practical and cost-effective implementation.

6.1.3. Material Performance Enhancement and Development of Novel Materials

To advance the development of large-scale DEGs, researchers must address several key areas of concern. Improving global

efficiency is a crucial goal, as it can lead to more efficient energy harvesting and reduce overall waste. This can be achieved by synthesizing improved dielectric materials with reduced electromechanical losses, increasing the energy conversion efficiency of DEGs. Additionally, research on low-carbon-footprint biodegradable polymers is needed, as sustainable and environmentally friendly materials are becoming increasingly important in all areas of technological development.

6.1.4. Modeling Tools

The development of sophisticated modeling tools is crucial for advancing the science of dielectric elastomers. Current modeling tools do not fully capture the complexities of environmental sensitivity and electromechanical coupling effects. Accurate simulation of material behavior, nonlinear electrical effects, and environmental interactions is necessary to optimize DEG design and performance. Future research should focus on developing comprehensive software tools that integrate these factors, enabling better prediction and analysis of DEG behavior under various conditions. Such tools would facilitate the design of novel materials and improve the selection and optimization of DEGs for different applications.

6.1.5. Low-Voltage Operation

Reducing the operating voltage of DEGs is essential for enhancing safety, particularly in wearable devices. Current DEGs often require high voltages, which can pose safety risks. Researchers are exploring ways to produce dielectric materials with high permittivity at micrometer thicknesses to enable low-voltage operation. However, achieving low-voltage functionality also requires the development of compact and cost-effective step-down electronics. Advancements in power management technologies and the integration of efficient voltage regulation circuits will be necessary to ensure the safe and effective use of small-scale DEGs in consumer electronics and wearable applications.

6.1.6. Power Density

Balancing power density with stretchability is a key challenge in the development of stretchable energy harvesting devices. While increased stretchability often results in lower power densities due to the predominance of inactive materials, there is a need for devices that offer both high power density and flexibility. Researchers should focus on creating compact and efficient stretchable devices by optimizing material composition and device architecture. Developing new materials with high electromechanical activity and innovative designs that maximize the active material volume can help overcome the tradeoff between power density and stretchability, opening new application avenues.

6.1.7. Working Conditions

DEGs must perform reliably under various environmental conditions, including mechanical stresses and electrical loads. Encapsulation techniques are being investigated to protect DEG systems from adverse environmental factors, but these methods may still impact device longevity. To enhance the reliability and robustness of DEGs, researchers need to develop materials that can endure diverse environmental conditions, such as temperature extremes, humidity, and mechanical wear. Improved encapsulation materials and designs that offer better protection against environmental stresses will be essential for extending the operational lifespan and performance of DEGs.

6.1.8. Future Prospects

Advancements in Materials: Future research should prioritize the development of advanced dielectric materials with superior properties. Innovations in material science, such as the creation of new polymer blends, conductive fillers, and nanocomposites, can enhance the performance of DEGs. Research into materials with higher energy densities, better mechanical properties, and increased environmental stability will be critical for advancing DEG technology. Additionally, the development of sustainable materials, including biodegradable and low-carbon-footprint polymers, will align with global environmental goals and support the broader adoption of DEGs.

Improved Power Electronics: The advancement of power electronics is crucial for the practical application of DEGs. Future research should focus on developing more efficient and cost-effective high-voltage circuits, energy storage solutions, and power management systems. Innovations in power electronics that address current limitations, such as high voltage requirements and cost, will improve the practicality and commercial viability of DEGs. Enhanced power electronics will enable better integration of DEGs into various applications, from small-scale consumer electronics to large-scale energy harvesting systems.

Improved Electrode Materials: Future research on electrode materials for DEGs should prioritize the development of ultra-flexible, highly conductive electrodes that can maintain performance under extreme mechanical deformations, such as high-strain cycling and long-term fatigue. Exploring new material systems, like nanostructured conductive polymers, graphene-based composites, or LMs, could provide enhanced

electrical stability and reduced energy loss. Additionally, investigating the integration of self-healing mechanisms within the electrode materials could greatly improve their lifespan and reliability in dynamic applications. Emphasis should also be placed on developing more sustainable, scalable, and cost-effective electrode manufacturing processes to enable broader adoption of DEGs in real-world energy harvesting scenarios.

Enhanced Energy Conversion Techniques: Optimizing energy conversion techniques is essential for maximizing the efficiency of DEGs. Future work should focus on refining DEG designs, exploring new deformation modes, and improving interfacing circuits. Advanced modeling and simulation tools can aid in the development of more effective energy conversion strategies. By improving the efficiency of the energy conversion process, researchers can enhance the overall performance of DEGs and expand their applications.

Integration Strategies: Developing effective integration strategies for DEGs is vital for their practical use. This involves creating methods for attaching DEGs to complex structures and ensuring compatibility with existing systems. Innovative integration techniques that allow DEGs to be seamlessly incorporated into various applications, such as wearable devices and structural health monitoring systems, will facilitate their broader adoption. Research into flexible and adaptive integration methods will support the integration of DEGs into diverse environments and applications.

Scalability and Commercialization: To achieve widespread adoption of DEGs, it is essential to address scalability and commercialization challenges. Research should focus on developing scalable manufacturing processes and evaluating the economic feasibility of large-scale production. Exploring diverse application areas, including renewable energy systems, consumer electronics, and wearable technology, can drive the commercial success of DEGs. By addressing these challenges, researchers can unlock the full potential of DEGs and promote their adoption in various industries.

Addressing these challenges and pursuing these future research directions will enable the development of more efficient, reliable, and practical DEGs. Continued innovation and investigation in these areas will pave the way for significant advancements in sustainable energy harvesting technologies.

7. Conclusion

This review provides a detailed comparison of various transduction techniques for harvesting energy from renewable sources. DE-based energy harvesting is one of the best approaches, according to our analysis, because of its high energy density, low cost, flexible design, and capacity for significant multiaxial mechanical deformation.

The review covers recent developments in the field of DEGs, including commercially available DE materials, novel elastomer materials, and their electromechanical characterization. Our observations indicate that acrylic-based elastomers have better conversion efficiency compared to others. However, natural rubber shows great promise due to its high energy density and durability. The review also discusses novel elastomer materials, such as electroactive polymers with conducting fillers and polymer blends, which have shown superior electromechanical properties

compared to commercially available elastomers. Furthermore, the review examines energy conversion circuits and interfacing circuits for DE-based energy harvesting and investigates their conversion efficiency. Recent interfacing circuits utilizing a buck converter type with MOSFET achieved a 50% conversion efficiency at a low bias voltage of 200–300 V.

The review also covers recent prototypes for human motion, wave energy, and wind energy harvesting. It can be concluded that prototypes for harvesting human motion show promise for small-scale applications, such as powering wearable devices like smartwatches, heart monitors, and wireless earphones. For large-scale applications, wave energy harvesters show the most promise for generating power in the range of a few kilowatts. Efforts are underway to improve their designs to enable power generation in the range of megawatts to make them more feasible. Despite the potential of DEGs, they face challenges such as low durability and conversion efficiency. Efforts are underway to enhance their mechanical properties through polymer blending, reduce priming voltage for wearable applications, and scale up for large-scale applications.

Abbreviations

DE	Dielectric elastomer
DEG	Dielectric elastomer generators
mWEC	Membrane wave energy converters
PZT	Lead zirconate titanate
VHB	Very high bond
MOSFET	Metal oxide semiconductor field effect transistor
TRL	Technology readiness level
VI	Vibro impact
PMN-PT	Lead magnesium niobate–lead titanate
BT	Barium titanate
DBP	Dibutyl phthalate
TiO ₂	Titanium oxide
PDMS	Polydimethylsiloxane
MDI	4,4 diphenylmethane diisocyanate
PU	Polyurethane
CCTO	Copper calcium titanate
PDA	Polydopamine
SEM	Scanning electron microscope
SBS	Styrene-butadiene-styrene
M3M	Methyl-3-mercaptopropionate
DMSO	Dimethyl silicone oil
Q–V	Charge–voltage
DC	Direct current
PVDF	Polyvinylidene fluoride
OPEX	Operational expenditure
CAPEX	Capital expenditure
LCOE	Levelized cost of energy
PTO	Power take-off
OWC	Oscillating water column
CD	Circularly deflated

Acknowledgements

M.H. and K.P. extend their sincere appreciation to the ASEM-DUO fellowship programme (South Korea) that helps to conduct the joint research between Swansea University, UK, and the Indian Institute of Technology Patna, India. M.H. and I.C. also acknowledge the funding by the Swansea Bay City Deal and the European Regional Development Fund through the Welsh European Funding Office. This study is also supported by EPSRC through the Supergen ORE Hub (EP/S000747/1), which has been awarded funding for the Flexible Fund project Submerged bi-axial fatigue analysis for flexible membrane Wave Energy Converters (FF2021-1036). This work is also funded by Sanad Aerotech and supported by the Advanced Research and Innovation Center (ARIC), which is jointly funded by Aerospace Holding Company LLC, a wholly-owned subsidiary of Mubadala Investment Company PJSC and Khalifa University for Science and Technology.

Conflict of Interest

The authors declare no conflict of interest.

Author Contributions

Krishna Veer Singh Gurjar: Conceptualization (equal); Data curation (lead); Formal analysis (lead); Methodology (lead); Validation (lead); Visualization (lead); Writing—original draft (lead). **Anup Sankar Sadangi:** Conceptualization (supporting); Data curation (supporting); Formal analysis (supporting); Investigation (supporting); Methodology (supporting); Validation (equal); Visualization (equal); Writing—original draft (supporting). **Ajeet Kumar:** Conceptualization (supporting); Formal analysis (supporting); Methodology (supporting); Validation (supporting); Visualization (supporting); Writing—original draft (equal). **Dilshad Ahmad:** Conceptualization (supporting); Data curation (supporting); Formal analysis (supporting); Investigation (equal); Methodology (equal); Validation (supporting); Visualization (equal); Writing—original draft (supporting). **Karali Patra:** Conceptualization (lead); Funding acquisition (lead); Investigation (supporting); Project administration (lead); Resources (lead); Supervision (lead); Visualization (lead); Writing—review & editing (lead). **Ieuan Collins:** Conceptualization (supporting); Formal analysis (supporting); Methodology (equal); Validation (supporting); Writing—review & editing (supporting). **Mokarram Hossain:** Conceptualization (supporting); Formal analysis (supporting); Investigation (supporting); Project administration (lead); Resources (lead); Supervision (equal); Visualization (equal); Writing—review & editing (lead). **Rafic M. Ajaj:** Conceptualization (supporting); Funding acquisition (lead); Project administration (supporting); Resources (supporting); Supervision (supporting); Writing—review & editing (supporting). **Yahya Zweiri:** Funding acquisition (supporting); Project administration (supporting); Supervision (supporting); Visualization (supporting); Writing—review & editing (supporting).

Keywords

dielectric elastomer generators, dielectric elastomers, electroactive polymers, electromechanical characterizations, energy harvesting, harvesting prototypes, interface circuits

Received: July 24, 2024

Revised: October 13, 2024

Published online:

- [1] T. Kober, H. W. Schiffer, M. Densing, E. Panos, *Energy Strategy Rev.* **2020**, *31*, 100523.
- [2] S. Chiba, M. Waki, *Sustainable Chem. Pharm.* **2020**, *15*, 100205.

- [3] D. G. Wakshume, M. Ł. Płaczek, *Electron* **2024**, *13*, 987.
- [4] X. Du, L. Du, X. Cai, Z. Hao, X. Xie, F. Wu, *Energy Convers. Manage.* **2022**, *253*, 115178.
- [5] Z. Xu, K. Bao, K. Di, H. Chen, J. Tan, X. Xie, Y. Shao, J. Cai, S. Lin, T. Cheng, E. Shiju, K. Liu, Z. L. Wang, *Adv. Sci.* **2022**, *9*, 2201098.
- [6] X. Du, L. Du, P. Li, X. Liu, Y. Han, H. Yu, K. Tao, L. Tang, *Nano Energy* **2023**, *111*, 108417.
- [7] R. Liu, L. He, X. Liu, S. Wang, L. Zhang, G. Cheng, *Sustainable Energy Technol. Assess.* **2023**, *59*, 103417.
- [8] S. K. Sahu, A. S. Sadangi, K. Patra, in *COMADEM*, Huddersfield, UK, Vol. 166, September **2020**, p. 1261.
- [9] C. Pan, D. Liu, M. J. Ford, C. Majidi, *Adv. Mater. Technol.* **2020**, *5*, 2000754.
- [10] C. Lagomarsini, C. Jean-Mistral, G. Lombardi, A. Sylvestre, *Smart Mater. Struct.* **2019**, *28*, 035003.
- [11] R. Kaltseis, C. Keplinger, S. J. Adrian Koh, R. Baumgartner, Y. F. Goh, W. H. Ng, A. Kogler, A. Tröls, C. C. Foo, Z. Suo, S. Bauer, *RSC Adv.* **2014**, *4*, 27905.
- [12] S. T. Fang, S. B. Wang, G. Q. Zhang, C. Wang, J. C. Xu, Z. Z. Wang, A. J. Feng, Z. J. Qiao, D. Yurchenko, Z. H. Lai, *Sci. China Technol. Sci.* **2023**, *66*, 1317.
- [13] Y. H. Zhang, A. Lee, C. H. Lee, *Sens. Actuators, A* **2024**, *370*, 115207.
- [14] G. Boccalero, S. Chesne, E. Mignot, N. Riviere, C. Jean-Mistral, *Smart Mater. Struct.* **2022**, *31*, 015006.
- [15] V. Vallem, Y. Sargolzaeiaval, M. Ozturk, Y. C. Lai, M. D. Dickey, *Adv. Mater.* **2021**, *33*, 2004832.
- [16] S. Zhou, M. Lallart, A. Erturk, *J. Sound Vib.* **2022**, *528*, 116886.
- [17] E. Brusa, A. Carrera, C. Delprete, *Actuators* **2023**, *12*, 457.
- [18] R. D. Kornbluh, R. Pelrine, H. Prahlad, A. Wong-Foy, B. McCoy, S. Kim, J. Eckerle, T. Low, *MRS Bull.* **2012**, *37*, 246.
- [19] A. T. Mathew, V. T. V. Khanh, M. D. Bin Mohamed Aliffi, C. Liu, S. J. A. Koh, *J. Intell. Mater. Syst. Struct.* **2020**, *31*, 152.
- [20] C. L. Zhang, Z. H. Lai, M. Q. Li, D. Yurchenko, *J. Sound Vib.* **2020**, *487*, 115616.
- [21] G. Thomson, Z. Lai, D. V. Val, D. Yurchenko, *J. Sound Vib.* **2019**, *442*, 167.
- [22] J. W. Zhang, *Int. J. Mech. Mater. Des.* **2022**, *18*, 587.
- [23] A. T. Mathew, C. Liu, T. Y. N. Ng, S. J. A. Koh, *Sens. Actuators, A* **2019**, *294*, 61.
- [24] I. A. Anderson, T. A. Gisby, T. G. McKay, B. M. O'Brien, E. P. Calius, *J. Appl. Phys.* **2012**, *112*, 041101.
- [25] T. Vu-Cong, C. Jean-Mistral, A. Sylvestre, *Electroact. Polym. Actuators Devices* **2013**, 8687, 86870H.
- [26] H. Lai, C. A. Tan, Y. Xu, in *IMECE2011-65973*, Denver, Colorado, USA, Vol. 2, November **2011**, p. 601.
- [27] T. McKay, P. Walters, J. Rossiter, B. O'Brien, I. Anderson, *Electroact. Polym. Actuators Devices* **2013**, 8687, 86870J.
- [28] T. McKay, Ph.D., Auckland Bioengineering Institute, New Zealand **2011**.
- [29] F. Carpi, I. Anderson, S. Bauer, G. Frediani, G. Gallone, M. Gei, C. Graaf, C. Jean-Mistral, W. Kaal, G. Kofod, M. Kollasche, R. Kornbluh, B. Lassen, M. Matysek, S. Michel, S. Nowak, B. O'Brien, Q. Pei, R. Pelrine, B. Rechenbach, S. Rosset, H. Shea, *Smart Mater. Struct.* **2015**, *24*, 105025.
- [30] C. L. Zhang, Z. H. Lai, G. Q. Zhang, D. Yurchenko, *Nonlinear Dyn.* **2020**, *102*, 1271.
- [31] R. D. Kornbluh, R. Pelrine, H. Prahlad, A. Wong-Foy, B. McCoy, S. Kim, J. Eckerle, T. Low, *Electroact. Polym. Actuators Devices* **2011**, 7976, 797605.
- [32] Y. Zhao, L. J. Yin, S. L. Zhong, J. W. Zha, Z. M. Dang, *IET Nanodielectrics* **2020**, *3*, 99.
- [33] Z. Suo, *Acta Mech. Solida Sin.* **2010**, *23*, 549.
- [34] L. J. Romasanta, M. A. Lopez-Manchado, R. Verdejo, *Prog. Polym. Sci.* **2015**, *51*, 188.
- [35] F. B. Madsen, A. E. Daugaard, S. Hvilsted, A. L. Skov, *Macromol. Rapid Commun.* **2016**, *37*, 378.
- [36] G. Moretti, S. Rosset, R. Vertechy, I. Anderson, M. Fontana, *Adv. Intell. Syst.* **2020**, *2*, 2000125.
- [37] S. Chiba, M. Waki, R. Kornbluh, R. Pelrine, *Electroact. Polym. Actuators Devices* **2008**, 6927, 692715.
- [38] I. Collins, M. Hossain, W. Dettmer, I. Masters, *Renewable Sustainable Energy Rev.* **2021**, *151*, 111478.
- [39] K. Di, K. Bao, H. Chen, X. Xie, J. Tan, Y. Shao, Y. Li, W. Xia, Z. Xu, E. Shiju, *Sustainability* **2021**, *13*, 9881.
- [40] R. Vertechy, M. Fontana, G. Stiubianu, M. Cazacu, *Electroact. Polym. Actuators Devices* **2014**, 9056, 90561R.
- [41] Z. Q. Song, K. Ohyama, S. Shian, D. R. Clarke, S. Zhu, *Smart Mater. Struct.* **2020**, *29*, 015018.
- [42] A. Kumar, K. Patra, M. Hossain, *Polym. Compos.* **2020**, *42*, 914.
- [43] Y. Chen, A. Lorenzo, G. Moretti, M. Fontana, R. Vertechy, *Smart Mater. Struct.* **2019**, *28*, 114001.
- [44] R. Van Kessel, B. Czech, P. Bauer, in *IEEE Power and Energy Society General Meeting*, San Diego, California, USA, Vol. 2012, IEEE July **2012**, p. 1.
- [45] Z. Liao, M. Hossain, X. Yao, *Mech. Mater.* **2020**, *144*, 103366.
- [46] M. Hossain, D. K. Vu, P. Steinmann, *Arch. Appl. Mech.* **2015**, *85*, 523.
- [47] W. Hu, S. N. Zhang, X. Niu, C. Liu, Q. Pei, *J. Mater. Chem. C* **2014**, *2*, 1658.
- [48] J. Zhang, Y. Wang, H. Chen, B. Li, *Int. J. Smart Nano Mater.* **2015**, *6*, 162.
- [49] W. Huang, G. Kang, *Polym. Test.* **2022**, *109*, 107557.
- [50] J. Qiang, H. Chen, B. Li, *Smart Mater. Struct.* **2012**, *21*, 025006.
- [51] P. Brochu, X. Niu, Q. Pei, *Electroact. Polym. Actuators Devices* **2011**, 7976, 797606.
- [52] S. Hunt, T. G. McKay, I. A. Anderson, *Appl. Phys. Lett.* **2014**, *104*, 2012.
- [53] A. L. Skov, L. Yu, *Adv. Eng. Mater.* **2018**, *20*, 1700762.
- [54] L. Yu, F. B. Madsen, S. Hvilsted, A. L. Skov, *RSC Adv.* **2015**, *5*, 49739.
- [55] G. Boccalero, C. Jean-Mistral, M. Castellano, C. Boragno, *Composites, Part B* **2018**, *146*, 13.
- [56] E. Cho, L. L. Y. Chiu, M. Lee, D. Naila, S. Sadanand, S. D. Waldman, D. Sussman, *Polymers* **2021**, *13*, 1831.
- [57] A. Kumar, D. Ahmad, K. Patra, M. Hossain, *J. Appl. Polym. Sci.* **2021**, *138*, 12.
- [58] Y. Jiang, S. Liu, M. Zhong, L. Zhang, N. Ning, M. Tian, *Nano Energy* **2020**, *71*, 104606.
- [59] A. Schmidt, P. Rothemund, E. Mazza, *Sens. Actuators, A* **2012**, *174*, 133.
- [60] S. Rosset, I. A. Anderson, *Front. Robot. AI* **2022**, *9*, 825148.
- [61] L. Zhang, F. Song, X. Lin, D. Wang, *Mater. Chem. Phys.* **2020**, *241*, 122373.
- [62] Y. Jiang, C. Tian, J. Yao, W. Wu, N. Ning, M. Tian, L. Zhang, *Chem. Eng. J.* **2022**, *439*, 135339.
- [63] W. Li, X. Liu, Y. Jiang, W. Wu, B. Yu, N. Ning, M. Tian, L. Zhang, *Nano Energy* **2022**, *104*, 107969.
- [64] B. Huang, Y. Yu, Y. Zhao, Y. Zhao, L. Dai, Z. Zhang, H. F. Fei, *J. Appl. Polym. Sci.* **2024**, *141*, e54983.
- [65] D. Guo, X. Liu, A. Zhang, M. Ruan, Z. Liu, Z. Wang, *J. Polym. Sci.* **2024**, *62*, 536.
- [66] F. Wang, W. Zhou, Y. He, Y. Lv, Y. Wang, Z. Wang, *Composites, Part A* **2024**, *181*, 108129.
- [67] Y. J. Ma, J. W. Wang, J. B. Yang, Z. L. Zhang, Y. Zhang, M. Y. Zhang, L. Tao, *Polym. Compos.* **2024**, *45*, 7039.
- [68] E. Bortot, R. Springhetti, G. DeBotton, M. Gei, *Procedia IUTAM* **2015**, *12*, 42.

- [69] E. Bortot, R. Springhetti, M. Gei, *J. Eur. Ceram. Soc.* **2014**, *34*, 2623.
- [70] G. Yin, Y. Yang, F. Song, C. Renard, Z. M. Dang, C. Y. Shi, D. Wang, *ACS Appl. Mater. Interfaces* **2017**, *9*, 5237.
- [71] T. Chen, L. Pan, M. Lin, B. Wang, L. Liu, Y. Li, J. Qiu, K. Zhu, *Polym. Test.* **2015**, *47*, 4.
- [72] A. Bele, C. Tugui, L. Sacarescu, M. Iacob, G. Stiubianu, M. Dascalu, C. Racles, M. Cazacu, *Mater. Des.* **2018**, *141*, 120.
- [73] Y. Yang, Z. S. Gao, M. Yang, M. S. Zheng, D. R. Wang, J. W. Zha, Y. Q. Wen, Z. M. Dang, *Nano Energy* **2019**, *59*, 363.
- [74] Y. Zhao, J. W. Zha, L. J. Yin, S. T. Li, Y. Q. Wen, Z. M. Dang, *Polymer* **2018**, *149*, 39.
- [75] M. Gong, F. Song, H. Li, X. Lin, J. Wang, L. Zhang, D. Wang, *RSC Adv.* **2021**, *11*, 19088.
- [76] Y. Adeli, T. Raman Venkatesan, R. Mezzenga, F. A. Nüesch, D. M. Opris, *ACS Appl. Polym. Mater.* **2024**, *6*, 4999.
- [77] C. Ellingford, R. Zhang, A. M. Wemyss, Y. Zhang, O. B. Brown, H. Zhou, P. Keogh, C. Bowen, C. Wan, *ACS Appl. Mater. Interfaces* **2020**, *12*, 7595.
- [78] A. F. Bin Ahmad Osman, S. Bin Zakaria, N. S. Binti Ramlée, N. H. Binti Asri, *Mater. Today Proc.* **2022**, *75*, 63.
- [79] G. Gallone, F. Galantini, F. Carpi, *Polym. Int.* **2010**, *59*, 400.
- [80] S. Risse, B. Kussmaul, H. Krüger, G. Kofod, *Adv. Funct. Mater.* **2012**, *22*, 3958.
- [81] J. Hubertus, J. Neu, S. Croce, G. Rizzello, S. Seelecke, G. Schultes, *ACS Appl. Mater. Interfaces* **2021**, *13*, 39894.
- [82] W. Zang, X. Liu, J. Li, Y. Jiang, B. Yu, H. Zou, N. Ning, M. Tian, L. Zhang, *Chem. Eng. J.* **2022**, *429*, 132258.
- [83] H. Ding, W. Zang, J. Li, Y. Jiang, H. Zou, N. Ning, M. Tian, L. Zhang, *Compos. Commun.* **2022**, *31*, 101132.
- [84] W. Zang, Y. Wang, W. Wu, J. Yao, X. Hao, B. Yu, D. Wu, P. F. Cao, Y. Jiang, N. Ning, M. Tian, L. Zhang, *ACS Nano* **2024**, *18*, 1226.
- [85] J. Yao, W. Zang, Y. Wang, B. Yu, Y. Jiang, N. Ning, M. Tian, *ACS Appl. Mater. Interfaces* **2024**, *16*, 11595.
- [86] A. S. Sadangi, S. K. Sahu, K. Patra, *IEEE Trans. Instrum. Meas.* **2020**, *69*, 5620.
- [87] P. K. Illenberger, S. Rosset, U. K. Madawala, I. A. Anderson, *IEEE Trans. Ind. Electron.* **2021**, *68*, 6982.
- [88] R. K. Sahu, K. Patra, S. Bhaumik, A. K. Pandey, D. K. Setua, *Appl. Mech. Mater.* **2015**, *789*, 837.
- [89] T. R. Huq, S. S. Williamson, in *IECON Proc. (Industrial Electronics Conf.)*, Vienna, Austria, Vol. 39, IEEE November **2013**, p. 6698.
- [90] D. Sun, K. Ohyama, S. Zhu, T. Qu, in *2022 Int. Conf. on Electrical Machines and Systems, ICEMS*, Chiang Mai, Thailand, Vol. 2, IEEE November **2023**, p. 1.
- [91] L. Eitzen, C. Graf, J. Maas, *Electroact. Polym. Actuators Devices* **2013**, *8687*, 86870P.
- [92] A. S. Sadangi, S. K. Sahu, K. Patra, in *Proc. of the 2nd Int. Conf. on Inventive Systems and Control, ICISC*, Coimbatore, India, Vol. 2, IEEE January **2018**, p. 413.
- [93] C. Graf, J. Hitzbleck, T. Feller, K. Clauberg, J. Wagner, J. Krause, J. Maas, *Electroact. Polym. Actuators Devices* **2013**, *8687*, 86870N.
- [94] H. C. Lo, E. Calius, I. Anderson, *Electroact. Polym. Actuators Devices* **2013**, *8687*, 86870E.
- [95] L. Ciarella, K. E. Wilson, A. Richter, I. A. Anderson, E.-F. M. Henke, in *IFAC-PapersOnLine*, Nantes, France, June **2022**, Vol. 55, p. 588.
- [96] P. Fan, H. Chen, *Appl. Phys. A* **2018**, *124*, 148.
- [97] J. B. Cao, E. Shi-Ju, Z. Guo, Z. Gao, H. P. Luo, *AIP Adv.* **2017**, *7*, 115117.
- [98] T. Hoffstadt, C. Graf, J. Maas, *Smart Mater. Struct.* **2013**, *22*, 094028.
- [99] J. Zhou, L. Jiang, R. Khayat, *EPL* **2016**, *115*, 27003.
- [100] R. K. Sahu, K. Patra, *Mech. Adv. Mater. Struct.* **2016**, *23*, 170.
- [101] L. J. Yin, J. Y. Pei, Q. K. Feng, J. Zhu, Z. M. Dang, in *IET Conf. Proc., Xi'an, China, November* **2023**, Vol. 2021, p. 1790.
- [102] W. Wang, P. He, S. Soekamtoputra, F. Ge, K. Choi, G. Kang, S. Kim, in *IEEE Int. Conf. on Electro Information Technology*, Maine, USA, Vol. 2011, IEEE May **2011**, p. 1.
- [103] K. C. Peiwan He, W. Wang, *J. Controlled Release* **2011**, *11*, 430.
- [104] P. Zanini, J. Rossiter, M. Homer, *Smart Mater. Struct.* **2017**, *26*, 035037.
- [105] H. Shea, S. Jin, A. Koh, I. Graz, J. Shintake, *Electromechanically Active Polymers*, Springer, Cham, Switzerland **2016**.
- [106] T. Ikegame, K. Takagi, T. Ito, H. Kojima, H. Yoshikawa, *Electroact. Polym. Actuators Devices* **2017**, *10163*, 1016331.
- [107] T. Vu-Cong, C. Jean-Mistral, A. Sylvestre, *Smart Mater. Struct.* **2013**, *22*, 025012.
- [108] J. Cao, G. Xu, E. Shiju, T. Zhao, Z. Gao, H. Luo, *AIP Adv.* **2020**, *10*, 115017.
- [109] T. Sakano, K. Ohyama, S. Zhu, M. Waki, S. Chiba, in *Proc. of Active and Passive Smart Structures and Integrated Systems XIV*, California, USA, Vol. 11376, April **2020**, p. 521.
- [110] T. McKay, B. O'Brien, E. Calius, I. Anderson, *Electroact. Polym. Actuators Devices* **2011**, *7976*, 79760B.
- [111] T. McKay, B. O'Brien, E. Calius, I. Anderson, *Appl. Phys. Lett.* **2010**, *97*, 2008.
- [112] R. Panigrahi, S. Mishra, A. K. Srivastava, S. Basu, in *2017 IEEE Energy Conversion Congress and Exposition, ECCE*, Cincinnati, Ohio, USA, Vol. 2017, October **2017**, p. 4741.
- [113] P. Illenberger, K. Takagi, H. Kojima, U. K. Madawala, I. A. Anderson, *IEEE Trans. Power Electron.* **2017**, *32*, 6904.
- [114] P. Zanini, J. Rossiter, M. Homer, *Electroact. Polym. Actuators Devices* **2016**, *9798*, 97980W.
- [115] E. Shiju, A. Liu, J. Cao, C. Ge, L. Jin, X. Jiang, in *2015 IEEE Int. Conf. on Mechatronics and Automation, ICMA*, China, YYY, Vol. 2, August **2015**, p. 1648.
- [116] R. Panigrahi, S. K. Mishra, *IEEE Trans. Power Electron.* **2018**, *33*, 2792.
- [117] C. Graf, T. Hoffstadt, J. Maas, in *ASME 2012 Conf. Smart Mater. Adapt. Struct. Intell. Syst. SMASIS*, Stone Mountain, Georgia, USA, Vol. 2, September **2012**, p. 909.
- [118] G. Rizzello, S. Seelecke, M. Homer, J. Rossiter, P. Rodrigues de Oliveira Zanini, in *Proc. Electroactive Polymer Actuators and Devices (EAPAD) XX*, Denver, Colorado, USA, Vol. 10594, March **2018**, p. 315.
- [119] H. C. Lo, T. McKay, B. M. O'Brien, E. Calius, I. Anderson, *Electroact. Polym. Actuators Devices* **2011**, *7976*, 7976°C.
- [120] R. Pelrine, R. D. Kornbluh, Q. Pei, in *Proc. of Electroactive Polymer Actuators and Devices (EAPAD) XX*, Denver, Colorado, USA, Vol. 1059406, March **2018**, p. 15.
- [121] G. Kang, K. S. Kim, S. Kim, *Rev. Sci. Instrum.* **2011**, *82*, 046101.
- [122] J. Zhou, L. Jiang, R. E. Khayat, *J. Appl. Phys.* **2017**, *121*, 184102.
- [123] F. Ge, W. Wang, N. H. Gupte, K. Choi, G. Kang, S. Kim, in *2011 IEEE Green Technologies Conf.*, Green, Batonrouge, Louisiana, USA, Vol. 2011, IEEE April **2011**, p. 1.
- [124] P. He, F. Ge, W. Wang, K. Choi, G. Kang, S. Kim, in *IEEE Int. Conf. on Electro Information Technology*, Mankato, Maine, USA, IEEE May **2011**, p. 1.
- [125] T. G. McKay, B. M. O'Brien, E. P. Calius, I. A. Anderson, *Appl. Phys. Lett.* **2011**, *98*, 142903.
- [126] P. Zanini, J. Rossiter, M. Homer, *Electroact. Polym. Actuators Devices* **2017**, *10163*, 101631C.
- [127] S. Chiba, M. Waki, T. Wada, Y. Hirakawa, K. Masuda, T. Ikoma, *Appl. Energy* **2013**, *104*, 497.
- [128] L. Eitzen, C. Graf, J. Maas, *Electroact. Polym. Actuators Devices* **2012**, *8340*, 834018.
- [129] L. Jiang, C. C. Mi, S. Li, C. Yin, J. Li, *IEEE Trans. Power Electron.* **2013**, *28*, 4885.

- [130] C. Graf, J. Maas, D. Schapeler, in *Proc. of the 2010 IEEE Int. Conf. on Solid Dielectrics, ICSD*, Bologna, Piscataway, Italy, Vol. 10, July 2010, p. 1.
- [131] R. Panigrahi, S. K. Mishra, A. K. Srivastava, S. Basu, *IEEE Trans. Ind. Electron.* **2019**, 66, 3507.
- [132] L. Eitzen, C. Graf, J. Maas, in *IECON Proc. (Industrial Electronics Conf.)*, Piscataway, New Jersey, USA, Vol. 2011, November 2011, p. 1226.
- [133] L. Eitzen, C. Graf, J. Maas, in *IEEE Energy Conversion Congress and Exposition: ECCE, Proc.*, Phoenix, Arizona, USA, Vol. 2011, September 2011, p. 897.
- [134] G. Moretti, G. P. R. Papini, M. Righi, D. Forehand, D. Ingram, R. Vertechy, M. Fontana, *Smart Mater. Struct.* **2018**, 27, 035015.
- [135] T. Li, S. Qu, W. Yang, *J. Appl. Phys.* **2012**, 112, 034119.
- [136] P. Brochu, H. Stoyanov, X. Niu, Q. Pei, *Electroact. Polym. Actuators Devices* **2012**, 8340, 83401W.
- [137] G. Moretti, M. Santos Herran, D. Forehand, M. Alves, H. Jeffrey, R. Vertechy, M. Fontana, *Renewable Sustainable Energy Rev.* **2020**, 117, 109430.
- [138] S. J. A. Koh, C. Keplinger, R. Kaltseis, C.-C. Foo, R. Baumgartner, S. Bauer, Z. Suo, *J. Mech. Phys. Solids* **2017**, 105, 81.
- [139] D. Ahmad, S. K. Sahu, K. Patra, *Polym. Test.* **2019**, 79, 106038.
- [140] R. K. Sahu, K. Patra, *J. Inst. Eng. India: Ser. C* **2014**, 95, 207.
- [141] M. Pharr, J. Y. Sun, Z. Suo, *J. Appl. Phys.* **2012**, 111, 104114.
- [142] C. Jean-Mistral, M. Beaune, T. Vu-Cong, A. Sylvestre, *Electroact. Polym. Actuators Devices* **2014**, 9056, 90561H.
- [143] C. Chiang Foo, S. Jin Adrian Koh, C. Keplinger, R. Kaltseis, S. Bauer, Z. Suo, *J. Appl. Phys.* **2012**, 111, 094107.
- [144] Z. Wang, C. Xiang, X. Yao, P. Le, J. Mendez, Z. Suo, *PNAS* **2019**, 116, 5967.
- [145] W. Fan, Y. Wang, S. Cai, *Polym. Test.* **2017**, 61, 373.
- [146] P. Fan, H. Chen, *Polymers* **2018**, 10, 1341.
- [147] Y. Chen, L. Agostini, G. Moretti, M. Fontana, Y. Chen, L. Agostini, G. Moretti, G. Berselli, in *Proc. of Electroactive Polymer Actuators and Devices (EAPAD) XXI*, Denver, Colorado, USA, Vol. 10966, March 2019, p. 158.
- [148] T. Rey, G. Chagnon, J. B. Le Cam, D. Favier, *Polym. Test.* **2013**, 32, 492.
- [149] Y. Chen, L. Agostini, G. Moretti, M. Fontana, R. Vertechy, *Smart Mater. Struct.* **2018**, 28, 114001.
- [150] D. Ahmad, R. M. Ajaj, *Polym. Test.* **2021**, 106, 107408.
- [151] F. D'Amico, G. Carbone, M. M. Foglia, U. Galietti, *Eng. Fract. Mech.* **2013**, 98, 315.
- [152] M. Kroon, *Int. J. Solids Struct.* **2014**, 51, 4419.
- [153] D. Ahmad, M. S. Parancheerivilakkathil, A. Kumar, M. Goswami, R. M. Ajaj, K. Patra, M. Jawaid, K. Volokh, Y. Zweiri, *Polym. Test.* **2024**, 135, 108463.
- [154] C. Chen, Z. Wang, Z. Suo, *Extrem. Mech. Lett.* **2017**, 10, 50.
- [155] D. Ahmad, K. Patra, M. Hossain, *Continuum Mech. Thermodyn.* **2019**, 32, 489.
- [156] R. H. Lee, U. Basuli, M. Y. Lyu, E. S. Kim, C. Nah, *J. Appl. Polym. Sci.* **2014**, 131, 40076.
- [157] J. Cao, G. Lu, E. Shiju, Z. Gao, T. Zhao, W. Xia, *Sci. Rep.* **2021**, 11, 1.
- [158] R. Vertechy, M. Fontana, *Electroact. Polym. Actuators Devices* **2015**, 9430, 94300K.
- [159] C. Graf, J. Maas, *Smart Mater. Struct.* **2012**, 21, 094001.
- [160] W. Wu, Y. Jiang, M. Zhong, S. Liu, B. Yu, N. Ning, M. Tian, L. Zhang, *Compos. Sci. Technol.* **2022**, 228, 109639.
- [161] S. Chiba, M. Waki, M. Takeshita, K. Ohyama, *Smart Mater. Struct.* **2024**, 33, 065016.
- [162] C. Graf, J. Maas, D. Schapeler, in *Electroactive Polymer Actuators and Devices (EAPAD) 2010*, California, USA, Vol. 7642, SPIE April 2010, p. 764217.
- [163] C. Y. Rozaidy, M. N. M. K. Fakhzan, M. M. A. K. Mohamed, N. A. M. Amin, *J. Telecommun. Electron. Comput. Eng.* **2018**, 10, 113.
- [164] D. Xu, S. Michel, T. McKay, B. O'Brien, T. Gisby, I. Anderson, *Sens. Actuators, A* **2015**, 232, 195.
- [165] G. Thomson, D. Yurchenko, D. V. Val, Z. Zhang, *Energy Convers. Manage.* **2019**, 196, 1445.
- [166] T. Vu-Cong, C. Jean-Mistral, A. Sylvestre, *Electroact. Polym. Actuators Devices* **2013**, 8687, 86871S.
- [167] A. Kumar, A. S. Sadangi, K. Patra, A. T. Mathew, D. Ahmad, A. Saini, *IEEE Trans. Dielectr. Electr. Insul.* **2023**, 30, 563.
- [168] L. Liu, H. Chen, J. Sheng, J. Zhang, Y. Wang, S. Jia, *Electroact. Polym. Actuators Devices* **2014**, 9056, 905634.
- [169] A. K. Pandey, A. Khurana, A. K. Sharma, *Eur. J. Mech. A/Solids* **2024**, 105, 105222.
- [170] M. Righi, R. Vertechy, M. Fontana, in *ASME 2014 Conf. on Smart Materials, Adaptive Structures and Intelligent Systems, SMASIS*, Newport, Rhode Island, USA, Vol. 46148, September 2014, p. V001T0A013.
- [171] G. Moretti, M. Fontana, R. Vertechy, *J. Intell. Mater. Syst. Struct.* **2015**, 26, 740.
- [172] Y. Wang, J. X. Zhou, X. H. Wu, B. Li, L. Zhang, *Chin. Phys. Lett.* **2013**, 30, 066103.
- [173] G. Moretti, R. Vertechy, M. Fontana, in *ASME 2013 Conf. on Smart Materials, Adaptive Structures and Intelligent Systems, SMASIS*, Snowbird, Utah, USA, Vol. 1, September 2014, p. 1.
- [174] T. Hanuhov, R. Brighenti, N. Cohen, *Smart Mater. Struct.* **2024**, 33, 055004.
- [175] W. Sikora, *Acta Mech. Autom.* **2023**, 17, 499.
- [176] A. Tutcuoglu, C. Majidi, *Appl. Phys. Lett.* **2014**, 105, 241905.
- [177] M. Hossain, D. K. Vu, P. Steinmann, *Comput. Mater. Sci.* **2012**, 59, 65.
- [178] Y. F. Goh, S. Akbari, T. V. Khanh Vo, S. J. A. Koh, *Soft Rob.* **2018**, 5, 675.
- [179] F. A. Mohd Ghazali, C. K. Mah, A. AbuZaiter, P. S. Chee, M. S. Mohamed Ali, *Sens. Actuators, A* **2017**, 263, 276.
- [180] A. T. Mathew, S. J. A. Koh, *Int. J. Smart Nano Mater.* **2017**, 8, 214.
- [181] A. T. Mathew, S. J. A. Koh, in *IEEE/ASME Int. Conf. on Advanced Intelligent Mechatronics, AIM*, Auckland, Newzealand, Vol. 2018, IEEE July 2018, p. 1366.
- [182] Y. Zhu, H. Wang, D. Zhao, J. Zhao, *Smart Mater. Struct.* **2011**, 20, 115022.
- [183] A. K. Srivastava, S. Basu, *Sens. Actuators, A* **2021**, 319, 112401.
- [184] I. A. Antoniadis, D. T. Venetsanos, F. G. Papaspyridis, *Smart Mater. Struct.* **2013**, 22, 104007.
- [185] J. W. Zhang, J. W. Chen, Z. Q. Ren, *J. Mech.* **2021**, 37, 184.
- [186] D. Zhao, Y. Yin, H. Du, J. Liu, *J. Sound Vib.* **2024**, 568, 118073.
- [187] E. Bortot, M. Gei, G. deBotton, *Meccanica* **2015**, 50, 2751.
- [188] F. Foerster, H. F. Schlaak, *Electroact. Polym. Actuators Devices* **2014**, 9056, 905637.
- [189] S. E. Chen, L. Deng, Z. C. He, E. Li, G. Y. Li, *Smart Mater. Struct.* **2016**, 25, 055017.
- [190] A. Bele, G. Stiubianu, S. Vlad, C. Tugui, C. D. Varganici, L. Matricala, D. Ionita, D. Timpu, M. Cazacu, *RSC Adv.* **2016**, 6, 8941.
- [191] Y. Zuo, Y. Ding, J. Zhang, M. Zhu, L. Liu, J. Zhao, *Polymers* **2021**, 13, 784.
- [192] Z. Xu, Z. Lv, C. Zhang, K. Wu, P. Morshuis, A. Claverie, in *Proc. of the 2024 IEEE 5th Int. Conf. on Dielectrics, ICD*, Toulouse, France, Vol. 5, IEEE June 2024, p. 1.
- [193] H. Wang, C. Wang, T. Yuan, *Appl. Phys. Lett.* **2012**, 101, 033904.
- [194] E. Bortot, M. Gei, *Extrem. Mech. Lett.* **2015**, 5, 62.
- [195] S. Priya, H. C. Song, Y. Zhou, R. Varghese, A. Chopra, S. G. Kim, I. Kanno, L. Wu, D. S. Ha, J. Ryu, R. G. Polcawich, *Energy Harvesting Syst.* **2019**, 4, 3.

- [196] H. Liu, J. Zhong, C. Lee, S. W. Lee, L. Lin, *Appl. Phys. Rev.* **2018**, *5*, 041306.
- [197] M. Lallart, P. J. Cottinet, D. Guyomar, L. Lebrun, *J. Polym. Sci., Part B: Polym. Phys.* **2012**, *50*, 523.
- [198] J. Slade, in *Head- and Helmet-Mounted Displays XVII; and Display Technologies and Applications for Defense, Security, and Avionics VI*, Maryland, USA, Vol. 8383, April **2012**, p. 83830R.
- [199] S. Chiba, M. Waki, *Energies* **2022**, *15*, 5854.
- [200] R. Riemer, A. Shapiro, *J. Neuroeng. Rehabil.* **2011**, *8*, 1.
- [201] C. Jean-Mistral, S. Basrou, *Electroact. Polym. Actuators Devices* **2010**, *7642*, 764209.
- [202] X. Xie, S. Zheng, J. Tan, J. Cheng, J. Cai, Z. Xu, E. Shiju, *Adv. Mater. Technol.* **2024**, *9*, 2301172.
- [203] Z. Xu, J. Tan, H. Chen, K. Di, K. Bao, J. Cheng, X. Xie, S. Zheng, S. Lin, J. Cai, T. Cheng, L. Liu, Z. L. Wang, S. E, *Nano Energy* **2023**, *109*, 108314.
- [204] M. Waki, S. A. Chiba, K. Ohyama, S. Zhu, N. Oya, K. Fujita, *J. Mater. Sci. Eng., B* **2017**, *7*, 171.
- [205] S. Chiba, M. Waki, R. Kornbluh, R. Pelrine, *Smart Mater. Struct.* **2011**, *20*, 124006.
- [206] M. K. Hoffmann, G. Moretti, G. Rizzello, K. Flaßkamp, in *IFAC-PapersOnLine*, Nantes, France, June **2022**, Vol. 55, p. 546.
- [207] A. Pecher, J. P. Kofoed, *Handbook of Ocean Wave Energy*, Springer Open, Cham, Switzerland **2017**.
- [208] R. Vertechy, M. Fontana, G. P. Rosati Papini, D. Forehand, *Electroact. Polym. Actuators Devices* **2014**, *9056*, 90561G.
- [209] Y. Liu, L. Liu, Z. Zhang, Y. Jiao, S. Sun, J. Leng, *EPL* **2010**, *90*, 36004.
- [210] M. Waki, S. A. Chiba, Z. Song, S. Zhu, K. Ohyama, *J. Mater. Sci. Eng., B* **2017**, *7*, 179.
- [211] J. Maas, C. Graf, in *ASME 2011 Conf. on Smart Materials, Adaptive Structures and Intelligent Systems, SMASIS*, Scottsdale, Arizona, USA, Vol. 2, September **2011**, p. 435.
- [212] M. Righi, G. Moretti, D. Forehand, L. Agostini, R. Vertechy, M. Fontana, *Nonlinear Dyn.* **2021**, *105*, 2861.
- [213] G. Moretti, M. Fontana, R. Vertechy, *Meccanica* **2015**, *50*, 2797.
- [214] G. Moretti, G. Malara, A. Scialò, L. Daniele, A. Romolo, R. Vertechy, M. Fontana, F. Arena, *Renewable Energy* **2020**, *146*, 628.
- [215] G. Moretti, A. Scialò, G. Malara, G. G. Muscolo, F. Arena, R. Vertechy, M. Fontana, *Meccanica* **2021**, *56*, 1223.
- [216] S. Chiba, M. Waki, K. Fujita, K. Masuda, T. Ikoma, *J. Mater. Sci. Eng., B* **2017**, *7*, 39.
- [217] G. Pietro Rosati Papini, G. Moretti, R. Vertechy, M. Fontana, *Nonlinear Dyn.* **2018**, *92*, 181.
- [218] F. Arena, L. Daniele, V. Fiamma, M. Fontana, G. Malara, G. Moretti, A. Romolo, G. P. R. Papini, A. Scialò, R. Vertechy, in *Proc. of the Int. Conf. on Offshore Mechanics and Arctic Engineering—OMAE*, Madrid, Spain, Vol. 51319, June **2018**, p. V010T09A028.
- [219] G. P. R. Papini, R. Vertechy, M. Fontana, in *ASME 2013 Conf. on Smart Materials, Adaptive Structures and Intelligent Systems, SMASIS*, Snowbird, Utah, USA, Vol. 56031, September **2013**, p. V001T03A038.
- [220] G. Moretti, G. P. R. Papini, L. Daniele, D. Forehand, D. Ingram, R. Vertechy, M. Fontana, *Proc. R. Soc. A* **2019**, *475*, 20180566.
- [221] R. Vertechy, G. Pietro Papini Rosati, M. Fontana, *J. Vib. Acoust. Trans. ASME* **2015**, *137*, 011004.
- [222] P. Jean, A. Watzte, G. , C. Melis, R. Van Kessel, A. Fourmon, E. Barrabino, J. Heemskerk, J. P. Queau, *Electroact. Polym. Actuators Devices* **2012**, *8340*, 8340C.
- [223] D. Yurchenko, D. V. Val, Z. H. Lai, G. Gu, G. Thomson, *Smart Mater. Struct.* **2017**, *26*, 105001.
- [224] D. Yurchenko, Z. H. Lai, G. Thomson, D. V. Val, R. V. Bobryk, *Appl. Energy* **2017**, *208*, 456.
- [225] Z. H. Lai, G. Thomson, D. Yurchenko, D. V. Val, E. Rodgers, *Mech. Syst. Signal Process.* **2018**, *107*, 105.
- [226] M. Wu, J. Zhang, H. Wu, *Int. J. Mech. Sci.* **2024**, *265*, 108906.
- [227] Z. H. Lai, J. L. Wang, C. L. Zhang, G. Q. Zhang, D. Yurchenko, *Energy Convers. Manage.* **2019**, *199*, 111993.
- [228] T. G. McKay, S. Rosset, I. A. Anderson, H. Shea, *Smart Mater. Struct.* **2015**, *24*, 15014.
- [229] G. Moretti, M. Righi, R. Vertechy, M. Fontana, *Polymers* **2017**, *9*, 283.
- [230] C. Graf, J. Maas, *Electroact. Polym. Actuators Devices* **2011**, *7976*, 79760H.
- [231] J. Huang, S. Shian, Z. Suo, D. R. Clarke, *Adv. Funct. Mater.* **2013**, *23*, 5056.
- [232] P. Zanini, J. Rossiter, M. Homer, *Appl. Phys. Lett.* **2015**, *107*, 153906.
- [233] T. McKay, B. O'Brien, E. Calius, I. Anderson, *Smart Mater. Struct.* **2010**, *19*, 055025.
- [234] R. Kaltseis, C. Keplinger, S. J. Adrian Koh, R. Baumgartner, Y. F. Goh, H. N. Wee, A. Kogler, A. Tröls, C. C. Foo, Z. Suo, S. Bauer, *RSC Adv.* **2014**, *4*, 27905.
- [235] T. Vu-Cong, C. Jean-Mistral, A. Sylvestre, *Smart Mater. Struct.* **2012**, *21*, 105036.
- [236] A. Kumar, K. Patra, *Eng. Sci. Technol. Int. J.* **2021**, *24*, 1347.
- [237] J. Huang, S. Shian, Z. Suo, D. R. Clarke, *Electroact. Polym. Actuators Devices* **2013**, *8687*, 86870Q.
- [238] Y. Wang, B. Chen, Y. Bai, H. Wang, J. Zhou, *Appl. Phys. Lett.* **2014**, *104*, 064101.
- [239] J. Maas, C. Graf, *Smart Mater. Struct.* **2012**, *21*, 064006.
- [240] J. Due, S. Munk-Nielsen, R. Nielsen, in *IET Conf. Publications*, Brighton, UK, Vol. 2010, April **2010**, p. 244.
- [241] C. Graf, J. Hitzbleck, T. Feller, K. Clauberg, J. Wagner, J. Krause, J. Maas, *J. Intell. Mater. Syst. Struct.* **2014**, *25*, 951.
- [242] C. Graf, L. Eitzen, J. Maas, in *Proc. of the 2011 14th European Conf. on Power Electronics and Applications, EPE 2011*, Birmingham, UK, Vol. 14, September **2011**, p. 1.
- [243] A. S. Sadangi, A. Kumar, K. Patra, *IEEE Trans. Instrum. Meas.* **2022**, *71*, 1.
- [244] A. Kumar, D. Ahmad, K. Patra, *J. Phys.: Conf. Ser.* **2019**, *1240*, 012049.
- [245] M. Hossain, Z. Liao, *Addit. Manuf.* **2020**, *35*, 101395.
- [246] D. Ahmad, K. Patra, M. Hossain, A. Kumar, *Rubber Chem. Technol.* **2021**, *94*, 476.
- [247] S. Rosset, O. A. Araromi, H. R. Shea, *Extrem. Mech. Lett.* **2015**, *3*, 72.
- [248] Z. Liao, M. Hossain, X. Yao, R. Navaratne, G. Chagnon, *Polym. Test.* **2020**, *86*, 106478.
- [249] P. C. Binh, D. N. C. Nam, K. K. Ahn, *Mechatronics* **2014**, *24*, 1166.



Krishna Veer Singh Gurjar is currently pursuing his Ph.D. degree in mechanical engineering from the Department of Mechanical Engineering at the Indian Institute of Technology (IIT) Patna. His research focus includes electromechanical characterization of dielectric elastomers, dielectric elastomer-based energy harvesting, energy harvesting system design, and smart materials.



Anup Sankar Sadangi completed his Ph.D. degree in 2021 from the Department of Mechanical Engineering at the Indian Institute of Technology (IIT) Patna. Recently, he joined the Department of Electronic and Communication Engineering at Gayatri Vidya Parishad College of Engineering, Visakhapatnam, as an assistant professor. His research interests include the development of generators out of smart materials, electrical signal processing and control, and low-power circuits for energy harvesting and processing.



Ajeet Kumar completed his Ph.D. degree in 2020 from the Department of Mechanical Engineering at the Indian Institute of Technology (IIT) Patna. Recently, he joined the Department of Metallurgical and Materials Engineering at the Indian Institute of Technology (IIT) Roorkee as a postdoctoral fellow. His research interests include the synthesis and electrical characterizations of smart materials rubber composites for energy harvesting and processing.



Dilshad Ahmad completed his Ph.D. degree in 2020 from the Department of Mechanical Engineering at the Indian Institute of Technology (IIT) Patna. He joined the Department of Aerospace Engineering, Khalifa University of Science and Technology, Abu Dhabi, United Arab Emirates, as a postdoctoral researcher. His research interests include the characterization and fracture analysis of soft materials and morphing wings.



Karali Patra is a professor in the Department of Mechanical Engineering at the Indian Institute of Technology (IIT) Patna. His research focus includes micromachining, soft robotics, and smart materials. He has been listed among the top 2% of scientists worldwide (Stanford University, 2021).



Ieuan Collins completed his Ph.D. in 2022 from Zienkiewicz Institute for AI, Data, and Modelling at Swansea University. He recently joined Wave Energy Scotland as an Innovation engineer. His research interests include wave energy, flexible structures, and numerical modeling.



Mokarram Hossain is an associate professor in the Mechanical Engineering Staff of Zienkiewicz Institute for AI, Data, and Modelling at Swansea University. His research interests include soft materials, electro-active polymers, renewable energy, and numerical modeling.



Rafic M. Ajaj is an associate professor at the Department of Aerospace Engineering of Khalifa University of Science and Technology (KUST). He joined KUST in August 2019. Rafic is also a visiting academic in Aerospace Structures at the Aerodynamics and Flight Mechanics Group of the University of Southampton, UK. His research is mainly focused on morphing wings, aircraft/UAV design, flight mechanics, aeroelasticity, and adaptive structures.



Yahya Zweiri is a professor at the Department of Aerospace Engineering of Khalifa University of Science and Technology (KUST). He joined KUST in August 2019. He is currently the director of the Advanced Research and Innovation Center and professor of Aerospace Engineering at Khalifa University. His research focus is in the area of robotic systems for extreme conditions with particular emphasis on applied artificial intelligence (AI) aspects and neuromorphic vision systems.